



# Near-Optimal Distributed Band-Joins through Recursive Partitioning


Rundong Li\*

 Google, USA  
eadon.lee@gmail.com

Wolfgang Gatterbauer

 Northeastern University, USA  
w.gatterbauer@northeastern.edu

Mirek Riedewald

 Northeastern University, USA  
m.riedewald@northeastern.edu

## ABSTRACT

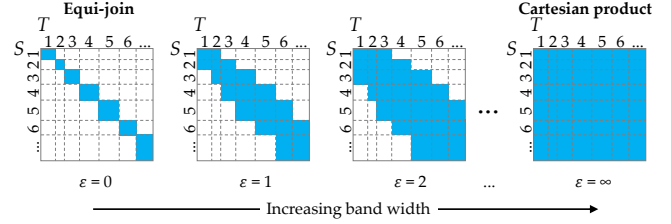
We consider running-time optimization for band-joins in a distributed system, e.g., the cloud. To balance load across worker machines, input has to be partitioned, which causes duplication. We explore how to resolve this tension between *maximum load per worker* and *input duplication* for band-joins between two relations. Previous work suffered from high optimization cost or considered partitionings that were too restricted (resulting in suboptimal join performance). Our main insight is that *recursive partitioning of the join-attribute space* with the appropriate split scoring measure can achieve both low optimization cost and low join cost. It is the first approach that is not only effective for one-dimensional band-joins but also for joins on multiple attributes. Experiments indicate that our method is able to find partitionings that are within 10% of the *lower bound* for both maximum load per worker and input duplication for a broad range of settings, significantly improving over previous work.

## KEYWORDS

band-join; distributed joins; running-time optimization

## 1 INTRODUCTION

Given two relations  $S$  and  $T$ , the band-join  $S \bowtie_B T$  returns all pairs  $(s \in S, t \in T)$  that are “close” to each other. Closeness is determined based on band-width constraints on the join attributes which we also call *dimensions*. This is related to (but in some aspects more general than, and in others a special case of) *similarity joins* (see Section 3). The Oracle Database SQL Language Reference guide [23] presents a one-dimensional (1D) example of a query finding employees whose salaries differ by at most \$100. Their discussion of band-join specific optimizations highlights the operator’s importance. Zhao et al [44] describe an astronomy application where celestial objects are matched using band conditions on time and coordinates *ra* (right ascension) and *dec* (declination). This type of approximate matching based on space and time is very common in practice and leads to three-dimensional (3D) band-joins like this:



**Figure 1: Join matrices for one-dimensional (1D) band-join  $|S.A - T.A| \leq \epsilon$  for increasing band width  $\epsilon$  from equi-join ( $\epsilon = 0$ ) to Cartesian product ( $\epsilon = \infty$ ). Numbers on matrix rows and columns indicate distinct  $A$ -values of input tuples. Cell  $(i, j)$  corresponds to attribute pair  $(s_i, t_j)$  and is shaded iff the pair fulfills the join condition and is in the output.**

**EXAMPLE 1.** Consider bird-observation table  $B$  with columns longitude, latitude, time, species, count, and weather table  $W$ , reporting precipitation and temperature for location-time combinations. A scientist studying how weather affects bird sightings wants to join these tables on attributes longitude, latitude, and time. Since weather reports do not cover the exact time and location of the bird sighting, she uses a band-join to link each bird report with weather data for “nearby” time and location, e.g.,  $|B.\text{longitude} - W.\text{longitude}| \leq 0.5$  AND  $|B.\text{latitude} - W.\text{latitude}| \leq 0.5$  AND  $|B.\text{time} - W.\text{time}| \leq 10$ .

We are interested in minimizing end-to-end running time of distributed band-joins, which is the sum of (1) *optimization time* (for finding a good execution strategy) and (2) *join time* (for the join execution). Join time depends on the *data partitioning* used to assign input records to worker machines. As seen in Figure 1, band-joins generalize equi-join and Cartesian product. Partitioning algorithms with optimality guarantees exist only for these two extremes [1, 25, 28].

**EXAMPLE 2.** To see why distributed band-joins are difficult, consider a 1D join with band width  $\epsilon = 1$  of  $S = \{1, 2, 3, 5, 6, 8, 9, 10\}$  and  $T = \{1, 5, 6, 10\}$  on  $w = 2$  workers. For balancing load, we may split  $S$  on value  $x$  and send the left half to worker  $w_1$  and the right half to  $w_2$  (see Figure 2a). To not miss results near the split point, all  $T$ -tuples within band width  $\epsilon = 1$  of  $x$  have to be copied across the boundary. Figure 2b shows the resulting input and output tuples on each worker, with duplicates in orange. By splitting in sparse regions

\*Work performed while PhD student at Northeastern University.

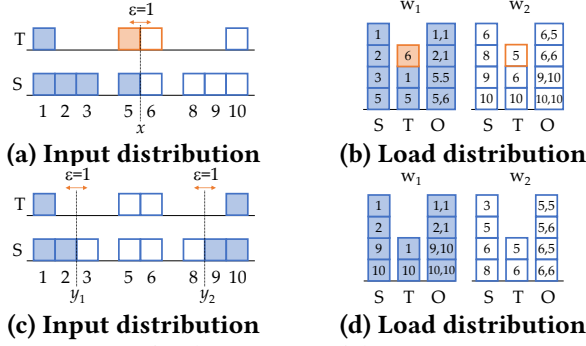


Figure 2: Input ( $S$ ,  $T$ ) and output ( $O$ ) on workers  $w_1$  and  $w_2$  when splitting on  $x$  (top row). The  $T$ -tuples shown in orange are duplicated because they are within the band width of the split point. When splitting on  $y_1$  and  $y_2$ , no tuple is duplicated and load is perfectly balanced (bottom row).

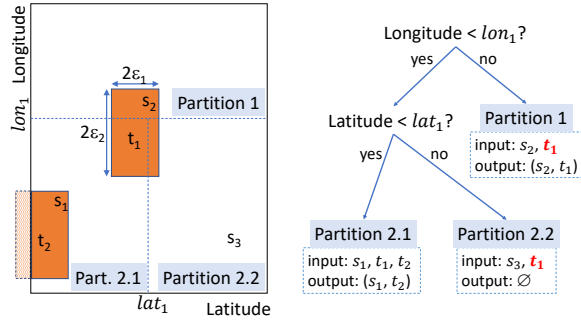


Figure 3: Recursive *split tree* for a 2D band-join on latitude and longitude. All splits are  $T$ -splits, i.e.,  $T$ -tuples within band width of the split boundary are sent to both children. For instance, at the root the  $\epsilon$ -range (orange box) of  $t_1$  crosses the  $lon_1$  line and therefore the tuple is copied to the right sub-tree (partition 1). The same happens again for the split on  $lat_1$ . This ensures that no match is missed (e.g.,  $(s_2, t_1)$ ) and no output tuple is produced twice.

of  $T$ , e.g., on  $y_1$  and  $y_2$  (Figures 2c and 2d), perfect load balance can be achieved without input duplication.

The main contribution of this work is a novel algorithm **REC**PART (**Recursive Partitioning**) that quickly and efficiently finds split points such as  $y_1$  and  $y_2$ . To do so, it has to carefully navigate the tradeoff between load balance and input duplication. For instance,  $y_1$  by itself appears like a poor choice from a load-balance point of view. It takes the additional split on  $y_2$  to unlock  $y_1$ 's true potential.

**Overview of the approach.** We propose recursive (i.e., hierarchical) partitioning of the join-attribute space, because it offers a broad variety of partitioning options that can be explored efficiently. As illustrated by the *split tree* in Figure 3, each path from the root node to a leaf defines a partition of the join-attribute space as a conjunction of the split predicates in the nodes along the path. Like *decision trees* in

machine learning [16], RECART's split tree is grown from the root, each time recursively splitting some leaf node. This step-wise expansion is a perfect solution for the problem of *navigating two optimization goals*: minimizing max worker load and minimizing input duplication. As RECART grows the tree, input duplication is monotonically increasing, because more tuples may have to be copied across a newly added split boundary. At the same time, large partitions are broken up and hence load balance may improve.

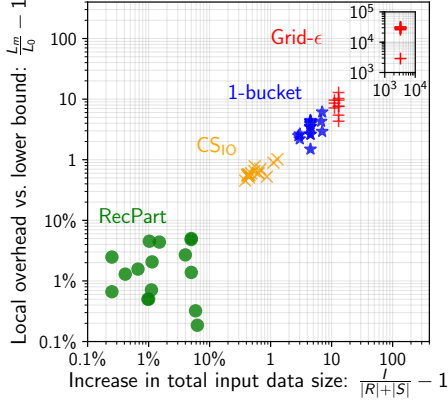
To find good partitionings, it is important to (1) use an appropriate scoring function to pick a good split point (e.g., choose  $y_1$  or  $y_2$  over  $x$  in Figure 2) and to (2) choose the best leaf to be split next. We propose the *ratio between load balance improvement and additional input duplication* for both decisions. In Example 2, this would favor  $y_1$  and  $y_2$  over  $x$ , because they add zero duplication. Similarly, a leaf node with a zero-duplicate split option would be preferred over a leaf whose split would cause duplication.

When a leaf becomes so small that virtually all tuples in the corresponding partition join with each other, then it is not split any further. However, if the load induced by that partition is high, then the leaf "internally" uses a grid-style partitioning inspired by 1-BUCKET [28] to create more fine-grained partitions. This is motivated by the observation that the band-join computation in a sufficiently small partition behaves like a Cartesian product—for which 1-BUCKET was shown to be near-optimal.

**Main contributions.** (1) We demonstrate analytically and empirically that previous work falls short either due to high optimization time (to find a partitioning) or due to high join time (caused by an inferior partitioning), especially for band-joins in more than one dimension.

(2) To address those shortcomings, we propose *recursive partitioning* of the multidimensional join-attribute space. Given a fixed-size input and output sample, our algorithm RECART finds a partitioning in  $O(w \log w + wd)$ , where  $w$  is the number of workers and  $d$  is the number of join attributes, i.e., the dimensionality of the band-join. RECART is inspired by decision trees [16], which had not been explored in the context of optimizing running time of distributed band-joins. To make them work for our problem, we identify a *new scoring measure* to determine the best split points: *ratio of load variance reduction to input duplication increase*. It is informed by our observation that a good split should improve load balance with minimal additional input duplication. We also identify a *new stopping condition* for tree growth.

(3) While we could not prove near-optimality of RECART's partitioning, our experiments provide strong empirical evidence. Across a variety of datasets, cluster sizes, and join conditions, RECART always found partitions for which both total input duplication and max worker load were within 10% of the corresponding *lower bounds*, beating all competitors



**Figure 4: Total input duplication (x-axis) and maximum overhead across workers (y-axis) for a variety of data points for our method RECPart vs. 3 competitors (see Section 6 for details). RECPart is always within 10% of the lower bounds (0% duplication and 0% overhead).**

(even those with significantly higher optimization cost) by a wide margin. Figure 4 shows this for a variety of problems (notice the log scale). The definition of the axes, the algorithms, and the detailed experiments are presented in Section 2, Section 3, and Section 6, respectively.

(4) We prove new Lemmas 2 and 3 that characterize when grid partitioning will be effective for distributed band-joins.

## 2 PROBLEM DEFINITION

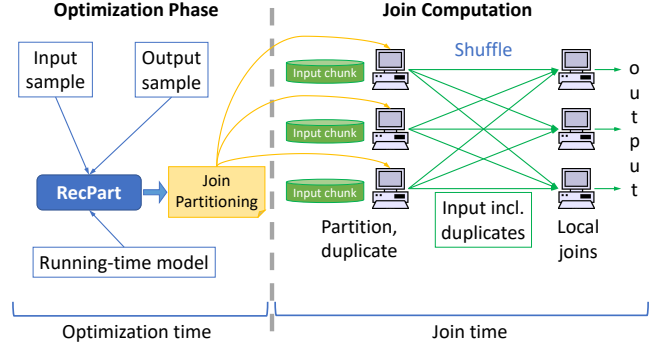
Without loss of generality, let  $S$  and  $T$  be two relations with the same schema  $(A_1, A_2, \dots, A_d)$ . Given a band width  $\varepsilon_i \geq 0$  for each attribute  $A_i$ , the band-join of  $S$  and  $T$  is defined as

$$S \bowtie_B T = \{(s, t) : s \in S \wedge t \in T \wedge \forall_{1 \leq i \leq d} |s.A_i - t.A_i| \leq \varepsilon_i\}.$$

We call  $d$  the *dimensionality* of the join and  $A_i$  the  $i$ -th *dimension*. We refer to the  $d$ -dimensional hyper-rectangle centered around a tuple  $a$  with side-length  $2\varepsilon_i$  in dimension  $i$ , formally  $\{(x_1, \dots, x_d) : \forall_{1 \leq i \leq d} a.A_i - \varepsilon_i \leq x_i \leq a.A_i + \varepsilon_i\}$ , as the  $\varepsilon$ -range around  $a$  (depicted as orange box in Figure 3). Note that  $(s, t)$  is in the output iff  $s$  falls into the  $\varepsilon$ -range around  $t$  (and vice versa). It is straightforward to generalize all results in this paper to asymmetric band conditions  $(a.A_i - \varepsilon_{i_L} \leq x_i \leq a.A_i + \varepsilon_{i_R})$  and to relations with attributes that do not appear in the join condition.

**DEFINITION 1 (JOIN PARTITIONING).** *Given input relations  $S$  and  $T$  with  $Q = S \bowtie_B T$  and  $w$  worker machines. A join partitioning is an assignment  $h : (S \cup T) \rightarrow 2^{\{1, \dots, w\}} \setminus \emptyset$  of each input tuple to one or more workers so that each join result  $q \in Q$  can be recovered by exactly one local join.*

A *local join* is the band-join executed by a worker on the input subset it receives. The definition ensures that *each output tuple is produced by exactly one worker*, which avoids



**Figure 5: Overview of the proposed approach.**

an expensive post-processing phase for duplicate elimination and is in line with previous work [1, 19, 28, 38].

Given  $S$ ,  $T$ , and a band-join condition, our goal is to minimize the time to compute  $S \bowtie_B T$ . This time is the sum of *optimization time* (i.e., the time to find a join partitioning) and *join time* (i.e., the time to compute the result based on this partitioning), as illustrated in Figure 5.

We follow common practice and define the load  $L_i$  on a worker  $w_i$  as the weighted sum  $L_i = \beta_2 I_i + \beta_3 O_i$ ,  $0 \leq \beta_2, 0 \leq \beta_3$  of input  $I_i$  and output  $O_i$  assigned to it [1, 25, 28, 38]. *Max worker load*  $L_m = \max_i L_i$  is the maximum load assigned to any worker. In addition, we also evaluate a partitioning based on its *total amount of input*  $I$ . It accounts for given inputs  $S$  and  $T$  and all duplicates created by the partitioning, i.e.,  $I = \sum_{x \in S \cup T} |h(x)|$ . Recall from Definition 1 that  $h$  assigns input tuples to a subset of the workers, i.e.,  $|h(x)|$  is the number of workers that receive tuple  $x$ .

**LEMMA 1 (LOWER BOUNDS).**  *$|S| + |T|$  is a lower bound for total input  $I$ . And  $L_0 = (\beta_2(|S| + |T|) + \beta_3|S \bowtie_B T|)/w$  is a lower bound for max worker load  $L_m$ .*

The lower bound for total input  $I$  follows from Definition 1, because each input tuple has to be examined by at least one worker. For max worker load, note that any partitioning has to distribute a total input of at least  $|S| + |T|$  and a total output of  $|S \bowtie_B T|$  over the  $w$  workers, for a total load of at least  $\beta_2(|S| + |T|) + \beta_3|S \bowtie_B T|$ .

**System Model and Measures of Success.** We consider the standard Hadoop MapReduce and Spark environment where inputs  $S$  and  $T$  are stored in files. These files may have been chunked up before the computation starts, with chunks distributed over the workers. Or they may reside in a separate cloud storage service such as Amazon’s S3. The files are not pre-partitioned on the join attributes and the workers do not have advance knowledge which chunk contains which join-attribute values. Hence any desired join partitioning requires that—in MapReduce terminology—(1) the entire input is read by map tasks and (2) a full shuffle is

performed to group the data according to the partitioning and have each group be processed by a reduce task.

In this setting, the shuffle time is determined by total input  $I$ , and the duration of the reduce phase (each worker performing local joins) is determined by max worker load. Hence we are interested in evaluating how close a partitioning comes to the lower bounds for total input and max worker load (Lemma 1). We use  $\frac{I - (|S| + |T|)}{|S| + |T|}$  and  $\frac{L_m - L_0}{L_0}$ , respectively, which measure by how much a value exceeds the lower bound, relative to the lower bound. For instance, for  $L_m = 11$  and  $L_0 = 10$  we obtain 0.1, meaning that the max worker load of the partitioning is 10% higher than the lower bound.

For systems with very fast networks, an emerging trend [2, 33], data transfer time is negligible compared to local join time, therefore the goal is to minimize max worker load, i.e., the success measure is  $\frac{L_m - L_0}{L_0}$ . In applications where the input is already *pre-partitioned on the join attributes* (e.g., for dimension-dimension array joins [11]) the optimization goal concentrates on reducing data movement [44]. There our approach can be used to *find the best pre-partitioning*, i.e., to chunk up the array on the dimensions.

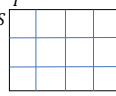
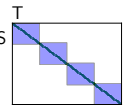
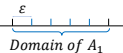
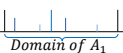
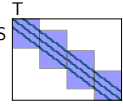
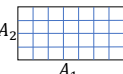

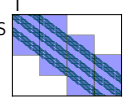
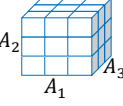
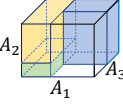
In addition to comparing to the lower bounds, we also measure end-to-end running time for a MapReduce/Spark implementation of the band-join in the cloud. For join-time estimation we rely on the model by Li et al. [24], which was shown to be sufficiently accurate to optimize running time of various algorithms, including equi-joins. Similar to the equi-join model, our band-join model  $\mathcal{M}$  takes as input triple  $(I, I_m, O_m)$  and estimates join time as a piecewise linear model  $\mathcal{M}(I, I_m, O_m) = \beta_0 + \beta_1 I + \beta_2 I_m + \beta_3 O_m$ . The  $\beta$ -coefficients are determined using linear regression on a small benchmark of training queries and inputs.

### 3 RELATED WORK

#### 3.1 Direct Competitors

Direct competitors are approaches that (1) support distributed band-joins and (2) optimize for load balance, i.e., max worker load or a similar measure. We classify them into *join-matrix covering* vs *attribute-space partitioning*.

**Join-matrix covering.** These approaches model distributed join computation as a covering problem for the *join matrix*  $J = S \times T$ , whose rows correspond to  $S$ -tuples and columns to  $T$ -tuples. A cell  $J(s, t)$  is “relevant” iff  $(s, t)$  satisfies the join condition. Any theta-join, including band-joins, can be represented as the corresponding set of relevant cells in  $J$ . A join partitioning can then be obtained by covering all relevant cells with non-overlapping regions. Since the exact set of relevant cells is not known a priori (it corresponds to the to-be-computed output), the algorithm covers a larger region of the matrix that is guaranteed to contain

Join-Matrix Covering		Attribute-Space Partitioning		$d$
1-BUCKET [28]	CS <sub>IO</sub> [38]	GRID- $\epsilon$ [9, 37]	RECPART	
				1
				2
				3

**Figure 6: Illustration of partitioning methods for band-joins in  $d$ -dimensional space for  $d = 1, 2, 3$ ; the  $A_i$  are the join attributes. GRID- $\epsilon$  and RECPART partition the  $d$ -dimensional join-attribute space, while CS<sub>IO</sub> and 1-BUCKET create partitions by finding a cover of the 2-dimensional join matrix  $S \times T$ , whose dimensions are independent of the dimensionality of the join condition. Bar height for RECPART and  $d = 1$  indicates recursive partition order.**

all relevant cells. For instance, for inequality predicates, M-Bucket-I [28] partitions both inputs on approximate quantiles in one dimension and then covers with  $w$  rectangles all regions corresponding to combinations of inter-quantile ranges from  $S$  and  $T$  that could potentially contain relevant cells. IEJoin [19] directly uses the same quantile-based range partitioning, but without attempting to find a  $w$ -rectangle cover. Its main contribution is a clever *in-memory* algorithm for queries with two join predicates. Optimizing local processing is orthogonal to our focus on how to *assign input tuples to multiple workers*. In fact, one can use an adaptation of their idea for local band-join computation on each worker.

To support any theta-join, 1-BUCKET [28] covers the entire join matrix with a grid of  $r$  rows and  $c$  columns. This is illustrated for  $r = 3$  and  $c = 4$  in Figure 6. Each  $S$ -tuple is randomly assigned to one of the  $r$  rows (which implies that it is sent to *all*  $c$  partitions in this row); this process is analogous for  $T$ -tuples, which are assigned to random columns. While randomization achieves near-perfect load balance, input is duplicated approximately  $\sqrt{w}$  times.

Zhang et al. [43] extend 1-BUCKET to joins between many relations. Koumarelas et al. [22] explore re-ordering of join matrix rows and columns to improve the running time of M-Bucket-I [28]. However, like M-Bucket-I, their technique does not take output distribution into account. This was shown to lead to poor partitionings by Vitorovic et al. [38]



whose method  $CS_{IO}$  represents the state of the art for distributed theta-joins. It relies on a carefully tuned optimization pipeline that first range-partitions  $S$  and  $T$  using approximate quantiles, then coarsens those partitions, and finally finds the optimal (in terms of max worker load) rectangle covering of the coarsened matrix. The resulting partitioning was shown to be superior—including for band-joins—to direct quantile-based partitioning, which is used by IEJoin. **Figure 6** illustrates  $CS_{IO}$  for a covering with four rectangles for 1, 2 and 3 dimensions. The darker diagonal “bands” show relevant matrix cells, i.e., cells that have to be covered. Notice how join dimensionality affects relevant-cell locations, but does not affect the dimensionality of the join matrix: *for a join between two input relations  $S$  and  $T$ , the join matrix is always two-dimensional, with one dimension per input relation.*

$CS_{IO}$  suffers from high optimization cost to find the covering rectangles, which uses a tiling algorithm of complexity  $O(n^5 \log n)$  for  $n$  input tuples. Optimization cost can be reduced by coarsening the statistics used. Further reduction in optimization cost is achieved for monotonic join matrices, a property that holds for 1-dimensional band-joins but *not for multidimensional ones*. As our experiments will show, the high optimization cost hampers the approach for multidimensional band-joins.

**Attribute-space partitioning.** Instead of using the 2-dimensional  $S \times T$  join matrix, attribute-space partitioning works in the  $d$ -dimensional space  $A_1 \times A_2 \times \dots \times A_d$  defined by the domains of the join attributes. Grid partitioning of the attribute space was explored in the early days of parallel databases, yet only for one-dimensional conditions. Soloviev [37] proposes the *truncating hash algorithm* and shows that it improves over a parallel implementation of the hybrid partitioned band-join algorithm by DeWitt et al. [9]. The method generalizes to more dimensions as illustrated in the GRID- $\epsilon$  column in **Figure 6**. Grid cells define partitions and are assigned to the workers.

By default, GRID- $\epsilon$  sets grid size for attribute  $A_i$  to the band width  $\epsilon_i$  in that dimension. This results in near-zero optimization cost, but may create a poor load balance (for skewed input) and high input duplication (when a partition boundary cuts through a dense region). A coarser grid reduces input duplication, but the larger partitions make load balancing more challenging. Our approach RECPART, which also applies attribute-space partitioning, mitigates the problem by considering recursive partitionings that avoid cutting through dense regions.

### 3.2 Other Related Work

**Similarity joins** are related to band-joins, but neither generalizes the other: the similarity joins closest to band-joins define a pair ( $s \in S, t \in T$ ) as similar if  $\text{sim}(s, t) > \theta$ , for some

similarity function  $\text{sim}$  and threshold  $\theta$ . This includes 1D band-joins as a special case, but does not support band-joins in multiple dimensions. (A band-join in  $d$  dimensions has  $2d$  threshold parameters for lower and upper limits in each dimension.) A recent survey [13] compares 10 distributed set-similarity join algorithms. The main focus of previous work on similarity joins is on addressing the specific challenges posed by working in a *general metric space* where vector-space operations such as addition and scalar multiplication (which band-joins can exploit) are not available. A particular focus is on (1) identifying fast filters that prune away a large fraction of candidate pairs without computing their similarity and (2) selecting pivot elements or anchor points to form partitions, e.g., via sampling [34].

Duggan et al [11] study skew-aware optimization for **distributed array equi-joins** (not band-joins). The work by Zhao et al [44] is closest to ours, because they introduce array similarity joins that can encode multi-dimensional band-join conditions. However, it is not a direct competitor for RECPART, because it considers a different optimization problem: The array is assumed to be already grid-partitioned into chunks on the join attributes and the main challenge is to co-locate with minimal network cost those partitions that need to be joined. Our approach is orthogonal for two reasons: First, we do not make any assumptions about existing pre-partitioning on the join attributes and hence the join requires a full data shuffle. Second, we show that for band-joins, grid partitioning is inferior to RECPART’s recursive partitioning. Hence RECPART provides new insights for choosing better array partitions when the array DBMS anticipates band-join queries.

**Attribute-space partitioning** is explored in other contexts for optimization goals that are very different from distributed band-join optimization. For array tiling, the goal is to minimize page accesses of range queries [14]. Here, like for histogram construction [31, 32], the band-join’s data duplication across a split boundary is not taken into account. Histogram techniques optimize for a different goal: maximizing the information captured with a given number of partitions. Only the equi-weight histograms by Vitorovic et al. [38] take input duplication into account. We include their approach  $CS_{IO}$  in our comparison.

For equi-joins, several algorithms address skew by **partitioning heavy hitters** [1, 4, 10, 26, 29, 30, 40, 41]. Other than the high-level idea of splitting up large partitions to improve load balance, the concrete approaches do not carry over to band-joins: They rely on the property that tuples with different join values cannot be matched, i.e., do not capture that tuples within band width of a split boundary must be duplicated. However, our decision to use load variance for measuring load balance was inspired by the state-of-the-art equi-join algorithm of Li et al. [25]. Earlier work relied on

---

**Algorithm 1: RECPART**


---

**Data:**  $S, T$ , band-join condition, sample size  $k$

**Result:** Hierarchical partitioning  $\mathcal{P}^*$  of  $A_1 \times \dots \times A_d$

```

1 Draw random input sample of size  $k/2$  from  $S$  and  $T$ 
2 Draw random output sample [38] of size  $k/2$ 
3 Initialize  $\mathcal{P}$  with root partition  $p_r = A_1 \times \dots \times A_d$ 
4  $p_r.\text{bestSplit}, \text{topScore} = \text{best\_split}(p_r)$ 
5 repeat
6   Let  $p \in \mathcal{P}$  be the leaf node with the highest topScore
7   Apply  $p.\text{bestSplit}$ 
8   foreach newly created (for regular leaf split) or updated (for
      small leaf split) leaf node  $p'$  do
9      $p'.(\text{bestSplit}, \text{topScore}) = \text{best\_split}(p')$ 
10 until termination condition
11 Return best partitioning  $\mathcal{P}^*$  found

```

---



---

**Algorithm 2: best\_split**


---

**Data:** Partition  $p$ , input and output sample tuples in  $p$ , number of row sub-partitions  $r$  and column sub-partitions  $c$  ( $r = c = 1$  for regular partitions)

**Result:** Split predicate bestSplit and its score topScore

```

1 Initialize topScore = 0 and bestSplit = NULL
2 if  $p$  is a regular partition then
3   // Find best decision-tree style split
4   foreach regular dimension  $A_i$  do
5     Let  $x_i$  be the split predicate on dimension  $A_i$  that has the
      highest ratio  $\sigma_i = \Delta\text{Var}(x_i)/\Delta\text{Dup}(x_i)$  among all possible
      splits in dimension  $A_i$ 
6     if  $\sigma_i > \text{topScore}$  then
7       Set topScore =  $\sigma_i$  and set bestSplit =  $x_i$ 
8 else
9   // Small partition: increment number of row or
      column sub-partitions using 1-Bucket
10  Let  $\sigma_r = \Delta\text{Var}(r+1, c)/\Delta\text{Dup}(r+1, c)$ 
11  Let  $\sigma_c = \Delta\text{Var}(r, c+1)/\Delta\text{Dup}(r, c+1)$ 
12  if  $\sigma_r > \sigma_c$  then
13    Set topScore =  $\sigma_r$  and set bestSplit = row
14  else
15    Set topScore =  $\sigma_c$  and set bestSplit = column
16 Return (bestSplit, topScore)

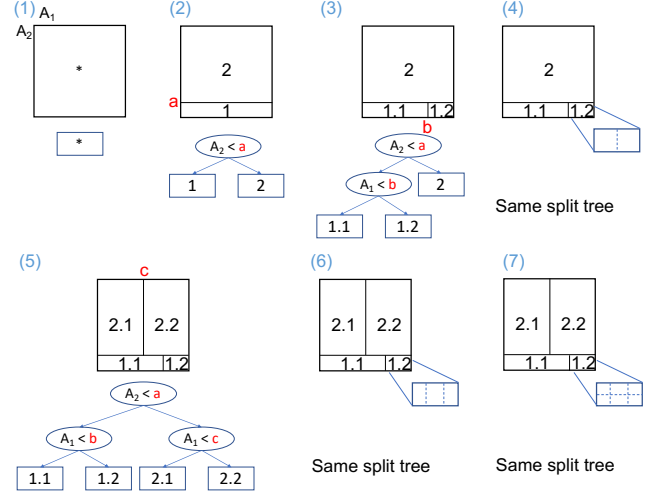
```

---

hash partitioning [8, 21] and focused on assigning partitions to processors [7, 12, 17, 18, 20, 33, 39]. Empirical studies of parallel and distributed equi-joins include [3, 5, 8, 35, 36].

## 4 RECURSIVE PARTITIONING

We introduce RECPART and analyze its complexity.



**Figure 7: Recursive partitioning for a 2D band-join on attributes  $A_1$  and  $A_2$ .** In the split tree, a path from the root to a leaf defines a rectangular partition in  $A_1 \times A_2$  as the conjunction of all predicates along the path. (By convention the left child is the branch satisfying the split predicate.) In small partitions such as 1.2, RECPART applies 1-BUCKET. Those partitions are terminal leaves in the split tree and only change their “internal” partitioning.

### 4.1 Main Structure of the Algorithm

RECPART (Algorithm 1) is inspired by decision trees [16] and recursively partitions the  $d$ -dimensional space spanned by all join attributes. To adapt this high-level idea to running-time optimization for band-joins, we (1) identify a new split-scoring measure that determines the selection of split boundaries, (2) propose a new stopping condition for the splitting process, and (3) propose an ordering to determine which tree leaf to consider next for splitting. The splitting process is illustrated in Figure 7.

Algorithm 1 starts with a single leaf node covering the entire join-attribute space and calls best\_split (Algorithm 2) on this leaf to find the best possible split and its score. Assuming the leaf is a “regular” partition (we discuss small partitions below), best\_split sorts the input sample on  $A_1$  and tries all middle-points between consecutive  $A_1$ -values as possible split boundaries. Then it does the same for  $A_2$ . The winning split boundary is the one with the highest ratio between load-variance reduction and input duplication increase (see details in Section 4.2).

Assume the best split is  $A_2 < a$ . The first execution of the repeat-loop then applies this split, creating new leaves “1” and “2” and finding the best split for each of them. Which leaf should be split next? RECPART manages all split-tree leaves in a priority queue based on their topScore value. Assuming leaf “1” has the higher score, the next repeat-loop iteration will

split it, creating new leaves “1.1” and “1.2”. This process continues until the appropriate termination condition is reached (discussed below). As the split tree is grown, the algorithm also keeps track of the best partitioning found so far.

## 4.2 Algorithm Details

**Small partitions.** When a partition becomes “small” relative to band width in a dimension, then no further *recursive* splitting in that dimension is allowed. When the partition is small in *all* dimensions, then it switches into a different partitioning mode inspired by 1-BUCKET [28]. This is motivated by the observation that when the length of a partition approaches band width in each dimension, then all  $S$  and  $T$ -tuples in that partition join with each other. And for Cartesian products, 1-BUCKET was shown to be near-optimal.

We define a partition as “small” as soon as its size is below twice the band width in all dimensions. In Figure 7 step (4), leaf “1.2” is small and hence when it is picked in the repeat-loop, applying the best split leaves the split tree unchanged, but instead increases the number of column partitions  $c$  to 2. Afterward, the topScore value of leaf “1.2” may have decreased and leaf “2” is split next, using a regular recursive split. This may be followed by more “internal” splits of leaf “1.2” in later iterations as shown in Figure 7, steps (6) and (7).

It is easy to show that having some leaves in “regular” and others in “small” split mode does not affect correctness. Intuitively, this is guaranteed because duplication only needs to be considered inside the region that is further partitioned, i.e., it does not “bleed” beyond partition boundaries.

**Split scoring.** In split score  $\Delta\text{Var}(x_i)/\Delta\text{Dup}(x_i)$  for a regular dimension (Algorithm 2),  $\Delta\text{Var}(x_i)$  is defined as follows: Let  $\mathcal{L}$  denote the set of split-tree leaves. Each (sub-partition in a) leaf corresponds to a region  $p$  in  $A_1 \times \dots \times A_d$ , for which we estimate input  $I_p$  and output  $O_p$  from the random samples drawn by Algorithm 1. The load induced by  $p$  is  $l_p = \beta_2 I_p + \beta_3 O_p$ . Load variance is computed as follows: Assign each leaf in  $\mathcal{L}$  to a randomly selected worker. Then per-worker load is a random variable  $\mathcal{P}$  (we slightly abuse notation to avoid notational clutter) whose variance can be shown to be  $\mathbb{V}[\mathcal{P}] = \frac{w-1}{w^2} \sum_{p \in \mathcal{L}} l_p^2$ . We analogously obtain  $\mathbb{V}(\mathcal{P}')$  for a partitioning  $\mathcal{P}'$  that results from splitting some leaf  $p' \in \mathcal{L}$  into sub-partitions  $p_1$  and  $p_2$  using predicate  $x_i$ . Then  $\Delta\mathbb{V}(x_i) = \mathbb{V}(\mathcal{P}') - \mathbb{V}(\mathcal{P})$ .  $\mathbb{V}(\mathcal{P}')$  can be computed from  $\mathbb{V}(\mathcal{P})$  in *constant* time by subtracting  $\frac{w-1}{w^2} l_{p'}^2$  and adding  $\frac{w-1}{w^2} (l_{p_1} + l_{p_2})^2$ .

The additional duplication caused by a split is obtained by estimating the number of  $T$ -tuples within band width of the new split boundary using the input sample. When multiple split predicates cause no input duplication, then the best split is the one with the greatest variance reduction among them.

The calculation of load variance and input duplication for “small” leaves is analogous.

The split score reflects our goal of reducing max worker load with minimal input duplication. For the former, load-variance reduction could be replaced by other measures, but precise estimation of input and output on the most loaded worker is difficult due to dynamic load balancing applied by schedulers at runtime. We therefore selected load variance as a scheduler-independent proxy.

**Termination condition and winning partitioning.** We propose a *theoretical* and an *applied* termination condition for the repeat-loop in Algorithm 1. For the theoretical approach, the winning partitioning is the one with the *lowest overhead over the lower bound in terms of both max worker load and input duplication*, i.e., the one with the minimal value of  $\max \left\{ \frac{I - (|S| + |T|)}{|S| + |T|}; \frac{L_m - L_0}{L_0} \right\}$ . It is easy to show that each iteration of the repeat-loop monotonically increases input  $I$ , because each new split boundary (regular leaf) and more fine-grained sub-partitioning (small leaf) can only increase the number of input duplicates. At the same time, the loop iteration may or may not decrease  $\frac{L_m - L_0}{L_0}$ . Hence repeat-loop iterations can be terminated as soon as  $\frac{I - (|S| + |T|)}{|S| + |T|}$  exceeds the smallest value of  $\frac{L_m - L_0}{L_0}$  encountered so far.

The theoretical approach only needs input and output samples, as well as an estimate of the relative impact of an input tuple versus an output tuple on join computation time. Input sampling is straightforward; for output sampling we use the method from [38]. If the output is large, it efficiently produces a large sample. If the output is small, then the output has negligible impact on join computation cost. The experiments show that we get good results when limiting sample size based on memory size and sampling cost to at most 5% of join time.

For estimating load impact, we run band-joins with different input and output sizes  $I$  and  $O$  on an individual worker and use linear regression to determine  $\beta_2$  and  $\beta_3$  in load function  $\beta_2 I + \beta_3 O$ . In our Amazon cloud cluster,  $\beta_2/\beta_3 \approx 4$ . Note that  $\beta_2$  and  $\beta_3$  tend to increase with input and output. For the lower bound, we use the smallest values, i.e., those obtained for scenarios where a node receives about  $1/w$  of the input (recall that  $w$  is the number of workers). This establishes a lower value for the lower bound, i.e., it is more challenging for RECPART to be close to it.

For the applied approach, we use the cost model as discussed in the end of Section 2. The winning partitioning is the one with the lowest running time predicted by the cost model. Repeat-loop iterations terminate when estimated join time bottoms out. We detect this based on a window of the join times over the last  $w$  repeat-loop iterations: loop execution terminates when improvement is below 1% (or join time even increased) over those last  $w$  iterations. (We chose

---

**Algorithm 3:** assign\_input

---

**Data:** Input tuple  $t \in T$ ; node  $p$  in split tree**Result:** Set of leaves to which  $t$  is copied

```

1 if  $p$  is a leaf then
2   | Return (1-BUCKET ( $t, p$ ))
3 else
4   if  $p$  is a  $T$ -split node then
5     for each child partition  $p'$  of  $p$  that intersects with the
6        $\varepsilon$ -range of  $t$  do
7       | assign_input( $t, p'$ )
8   else
9     Let  $p'$  be the child partition of  $p$  that contains  $t$ 
10    assign_input( $t, p'$ )

```

---

$w$  as window size because it would take at least one extra split per worker to break up each worker's load. This dovetails with the prioritization of leaves: The most promising leaves in terms of splitting up load with low input duplication overhead are greedily selected.)

**Extension: symmetric partitioning.** Like classic grid partitioning, RECPART as discussed so far treats inputs  $S$  and  $T$  differently: at an inner node in the split tree,  $S$  is partitioned (without duplication), while  $T$ -tuples near the split boundary are duplicated. For regions where  $S$  is sparse and  $T$  is dense, we want to reverse these roles. Consider Figure 2c, where  $y_1$  and  $y_2$  enabled a zero-duplication partitioning with perfect load balance. What if the input distribution was reversed in another region of the join-attribute space, e.g.,  $S' = \{21, 25, 26, 30\}$  and  $T' = \{21, 22, 23, 25, 26, 28, 29, 30\}$ ? Then no split in range 21 to 30 could avoid duplication of  $T'$ -tuples because for band width 1 at least one of the  $T'$ -values would be within 1 of the split point. In that scenario we want to reverse the roles of  $S'$  and  $T'$ , i.e., perform the partitioning on  $T'$  and the partition/duplication on  $S'$ .

For grid partitioning, it is not clear how to reverse the roles of  $S$  and  $T$  in some of the grid cells. For RECPART, this turns out to be easy. When exploring split options in a regular leaf (1-BUCKET in small partitions already treats both inputs symmetrically), Algorithm 2 computes the duplication for both cases: partition  $S$  and partition/duplicate  $T$  as well as the other way round. We call the former a  $T$ -split and the latter an  $S$ -split. The split type information is added to the corresponding node in the split tree.

Algorithm 3 is used to determine which tuples to assign to the sub-trees. (Only the version for  $T$ -tuples is shown; the one for  $S$ -tuples is analogous.) It is easy to show that for each result  $(s, t) \in S \bowtie_B T$ , exactly one leaf in the split tree receives both  $s$  and  $t$ .

### 4.3 Algorithm Analysis

RECPART has low complexity, resulting in low optimization time. Let  $\lambda$  denote the number of repeat-loop executions in Algorithm 1. Each iteration increases the number of leaves in the split tree by at most one. The algorithm manages all leaves in a priority queue based on the score returned by Algorithm 2. With a priority queue where inserts have constant cost and removal of the top element takes time logarithmic in queue size, an iteration of the repeat-loop takes  $O(\log \lambda)$  to remove the top-scoring leaf  $p$ . If  $p$  is regular, then it takes  $O(1)$  to create sub-partitions  $p_1$  and  $p_2$  and to distribute all input and output samples in  $p$  over them. (Sample size is bounded by constant  $k$ , a fraction of machine-memory size.) Checking if  $p_1$  and  $p_2$  are small partitions takes time  $O(d)$ . Then best\_split is executed, which for a regular leaf requires sorting of the input sample on each dimension and trying all possible split points, each a middle point between two consecutive sample tuples in that dimension. Since sample size is upper-bounded by a constant, the cost is  $O(d)$ . For a small leaf, the cost is  $O(1)$ . Finally, inserting  $p_1$  and  $p_2$  into the priority queue takes  $O(1)$ . In total, splitting a regular or small leaf has complexity  $O(d)$  and  $O(1)$ , respectively.

After  $\lambda$  executions of the repeat-loop in Algorithm 1, the next iteration has complexity  $O(\log \lambda + d)$ . Hence the total cost of  $\lambda$  iterations is  $O(\lambda \log \lambda + \lambda d)$ . In our experience, the algorithm will terminate after a number of iterations bounded by a small multiple of the number of worker machines. To see why, note that each iteration breaks up a large partition  $p$  and replaces it by two (for regular  $p$ ) or more (for small  $p$ ) sub-partitions. The split-scoring metric favors breaking up heavy partitions, therefore load can be balanced across workers fairly evenly as soon as the total number of partitions reaches a small multiple of the number of workers. This in turn implies for Algorithm 1, given samples of fixed size, a total complexity of  $O(w \log w + wd)$ .

## 5 ANALYTICAL INSIGHTS

We present two surprising results about the ability of grid partitioning to address load imbalances. For join-matrix covering approaches like CS<sub>IO</sub> that depend on the notion of a total ordering of the join-attribute space, we explore how to enumerate the multi-dimensional space.

### 5.1 Properties of Grid Partitioning

Without loss of generality, let  $S$  be the input that is partitioned and  $T$  be the input that is partitioned/duplicated.

**Input duplication.** With grid-size in each dimension set to the corresponding band width, the  $\varepsilon$ -range of a  $T$ -tuple intersects with up to 3 grid cells per dimension, for a total replication rate of  $O(3^d)$  in  $d$  dimensions. Can this exponential dependency on the dimensionality be addressed through



coarser partitioning? Unfortunately, for any non-trivial partitioning, asymptotically the replication rate is still at least  $O(2^d)$ . To construct the worst case, an adversary places all input tuples near the corner of a centrally located grid cell.

**Max worker load.** We now show an even stronger negative result, indicating that grid-partitioning is inherently limited in its ability to reduce max worker load, no matter the number of workers or the grid size. Consider a partitioning where one of the grid cells contains half of  $S$  and half of  $T$ . Does there exist a more fine-grained grid partitioning where none of the grid cells receives more than 10% of  $S$  and 10% of  $T$ ? One may be tempted to answer in the affirmative: just keep decreasing grid size in all dimensions until the target is reached. Unfortunately, this does not hold as we show next.

**LEMMA 2.** *If there exists an  $\epsilon$ -range in the join-attribute space with  $n$  tuples from  $T$ , then grid partitioning will create a partition with at least  $n$   $T$ -tuples, no matter the grid size.*

**PROOF.** For  $d = 1$  consider an interval of size  $\epsilon_1$  that contains  $n$   $T$ -tuples. If no split point partitions the interval, then the partition containing it has all  $n$   $T$ -tuples. Otherwise, i.e., if at least one split point partitions the interval, pick one of the split points inside the interval, say  $X$ , and consider the  $T$ -tuples copied to the grid cells adjacent to  $X$ . Since all  $T$ -tuples in an interval of size  $\epsilon_1$  are within  $\epsilon_1$  of  $X$ , both grid cells receive all  $n$   $T$ -tuples from the interval. It is straightforward to generalize this analysis to  $d > 1$ .  $\square$

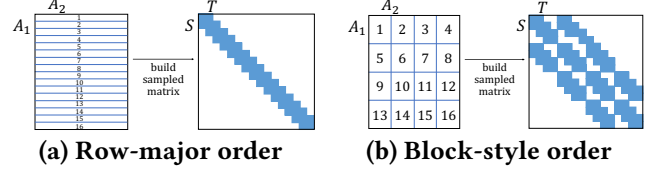
In short, even though a more fine-grained partitioning can split  $S$  into ever smaller pieces, the same is not possible for  $T$  because of the duplication needed to ensure correctness for a band-join. For *skewed* input,  $n$  in Lemma 2 can be  $O(|T|)$ . Interestingly, we now show that grid partitioning can behave well in terms of load distribution for skewed input, as long as the input is “sufficiently” large.

**LEMMA 3.** *Let  $c_0 > 0$  be a constant such that  $|S \bowtie_B T| \leq c_0(|S| + |T|)$ . Let  $R$  ( $R'$ ) denote the region of size  $\epsilon_1 \times \epsilon_2 \times \dots \times \epsilon_d$  in the join attribute space containing the most tuples from  $S$  ( $T$ ); and let  $x$  ( $x'$ ) and  $y$  ( $y'$ ) denote the fraction of tuples from  $S$  and  $T$ , respectively, it contains. If there exist constants  $0 < c_1 \leq c_2$  such that  $c_1 \leq x/y \leq c_2$  and  $c_1 \leq x'/y' \leq c_2$ , then no region of size  $\epsilon_1 \times \epsilon_2 \times \dots \times \epsilon_d$  contains more than  $O(\sqrt{1/|S| + 1/|T|})$  input tuples.*

**PROOF.** By definition, all  $S$  and  $T$  tuples in region  $R$  join with each other. Together with  $|S \bowtie_B T| \leq c_0(|S| + |T|)$  this implies

$$x|S| \cdot y|T| \leq c_0(|S| + |T|) \quad \Rightarrow \quad xy \leq c_0(1/|S| + 1/|T|) \quad (1)$$

From  $x/y \leq c_2$  follows  $x^2 \leq c_2xy$ , then  $x^2 \leq c_2c_0(1/|S| + 1/|T|)$  (from (1)) and thus  $x \leq \sqrt{c_0c_2}\sqrt{1/|S| + 1/|T|} =$



**Figure 8: Impact of enumeration order of a multidimensional space, here for a band-join between  $S$  and  $T$  on attributes  $A_1$  and  $A_2$ , on the location of cells in the join matrix that may produce output. Here band width is smaller than the height and width of each partition, resulting in a significantly sparser join matrix for row-major order.**

$O(\sqrt{1/|S| + 1/|T|})$ . We show analogously for region  $R'$  that  $y' \leq \sqrt{c_0/c_1}\sqrt{1/|S| + 1/|T|} = O(\sqrt{1/|S| + 1/|T|})$ .

Since  $R$  is the region of size  $\epsilon_1 \times \epsilon_2 \times \dots \times \epsilon_d$  with most  $S$ -tuples and  $R'$  the region with most  $T$ -tuples, no region of size  $\epsilon_1 \times \epsilon_2 \times \dots \times \epsilon_d$  can contain more than  $x$  fraction of  $S$ -tuples and  $y'$  fraction of  $T$ -tuples.  $\square$

**Lemma 3** is surprising. It states that for larger inputs  $S$  and  $T$ , the *fraction* of  $S$  and  $T$  in any partition of  $\text{GRID-}\epsilon$  (recall that its partitions are of size  $\epsilon_1 \times \epsilon_2 \times \dots \times \epsilon_d$ ) is upper-bounded by a function that decreases proportionally with  $\sqrt{|S|}$  and  $\sqrt{|T|}$ . For instance, when  $S$  and  $T$  double in size, then the upper bound on the input fraction in any partition decreases by a factor of  $\sqrt{2} \approx 1.4$ .

Clearly, this does not hold for all band joins. The proof of Lemma 3 required (1) that the region with most  $S$ -tuples contain a sufficiently large fraction of  $T$ , and vice versa; and (2) that output size is bounded by  $c_0$  times input size. The former is satisfied when  $S$  and  $T$  have a similar distribution in join-attribute space, e.g., a self-join. For the latter, we are aware of two scenarios. First, the user may actively try to avoid huge outputs by setting a smaller band width. Second, for any output-cost-dominated theta-join, 1-BUCKET was shown to be near-optimal [28]. Hence specialized band-join solutions such as RECPART, GRID- $\epsilon$ , and CS<sub>IO</sub> would only be considered when output is “sufficiently” small.

## 5.2 Ranges in Multidimensional Space

CS<sub>IO</sub> starts with a range partitioning of the join-attribute space based on approximate quantiles. For quantiles to be well-defined, a total order must be established on the multidimensional space—this was left unspecified for CS<sub>IO</sub>. The ordering can significantly impact performance as illustrated in Figure 8 for a 2D band-join. In row-major order, ranges correspond to long horizontal stripes. Alternatively, each range may correspond to a “block,” creating more square-shaped regions. This choice affects the candidate regions in the join matrix that need to be covered. Assume each horizontal stripe in Figure 8a is at least  $\epsilon_1$  high. Then an

$S$ -tuple in stripe  $i$  can only join with  $T$ -tuples in the three stripes  $i - 1$ ,  $i$ , and  $i + 1$ . This creates the compact candidate-region diagonal of width 3 in the join matrix. For the block partitioning in Figure 8b,  $S$ -tuples in a block may join with  $T$ -tuples in up to nine neighboring blocks. This creates the wider band in the join matrix. For CS<sub>IO</sub>, a wider diagonal and denser matrix cause additional input duplication.

In general, the number of candidate cells in the join matrix is minimized by row-major ordering, *if the distance between the hyperplanes in the most significant dimension is greater than or equal to the band width in that dimension*. This was the case in our experiments and therefore row-major ordering was selected for CS<sub>IO</sub>.

## 6 EXPERIMENTS

We compare the total running time (optimization plus join time) of RECPART to the state of the art (GRID- $\epsilon$ , CS<sub>IO</sub>, 1-BUCKET). Note that GRID- $\epsilon$  is not defined for band width zero. Reported times are measured on a real cloud, unless stated otherwise. In large tables, we mark cells with the main results in blue; red color highlights a weak spot, e.g., excessive optimization time or input duplication.

### 6.1 Experimental Setup

**Environments.** Both MapReduce [6] and Spark [42] are well-suited for band-join implementation. Spark’s ability to keep large data in memory makes little difference for the map-shuffle-reduce pipeline of a band-join, therefore we use MapReduce, where it is easier to control low-level behavior such as custom data partitioning. All experiments were conducted on Amazon’s Elastic MapReduce (EMR) cloud, using 30 m3.xlarge machines (15GB RAM, 40GB disk, high network performance) by default. All clusters run Hadoop 2.8.4 with the YARN scheduler in default configuration.

**Data.** For synthetic data, we use a Pareto distribution where join-attribute value  $x$  is drawn from domain  $[1.0, \infty)$  of real numbers and follows PDF  $z/x^{z+1}$  (greater  $z$  creates more skew). This models the famous power-law distribution observed in many real-world contexts, including the 80-20 rule for  $z = \log_4 5 \approx 1.16$ . We explore  $z$  in the range  $[0.5, 2.0]$ , which covers power-law distributions observed in real data. `pareto- $z$`  denotes a pair of tables, each with 200 million tuples, with Pareto-distributed join attributes for skew  $z$ . High-frequency values in  $S$  are also high-frequency values in  $T$ . `rv-pareto- $z$`  is the same as `pareto- $z$` , but high-frequency values in  $S$  have low frequency in  $T$ , and vice versa. Specifically,  $T$  follows a Pareto distribution from  $10^6$  down to  $-\infty$ . ( $T$  is skewed toward larger values. We generate  $T$  by drawing numbers from  $[1.0, \infty)$  following Pareto distribution and then converting each number  $y$  to  $10^6 - y$ .)

**Table 1: Band-join characteristics used in the experiments. Input and output size are reported in [million tuples].**

Data Set	$d$	Band width	Input Size	Output Size
pareto-1.5	1	0	400	2430
pareto-1.5	1	$10^{-5}$	400	4580
pareto-1.5	1	$2 \cdot 10^{-5}$	400	9120
pareto-1.5	1	$3 \cdot 10^{-5}$	400	11280
pareto-1.5	3	(0, 0, 0)	400	0
pareto-1.5	3	(2, 2, 2)	400	1120
pareto-1.5	3	(4, 4, 4)	400	8740
pareto-0.5	3	(2, 2, 2)	400	12
pareto-1.0	3	(2, 2, 2)	400	420
pareto-2.0	3	(2, 2, 2)	400	3200
pareto-1.5	8	(20, ..., 20)	100	9
pareto-1.5	8	(20, ..., 20)	200	57
pareto-1.5	8	(20, ..., 20)	400	219
pareto-1.5	8	(20, ..., 20)	800	857
rv- <code>pareto-1.5</code>	1	2	400	0
rv- <code>pareto-1.5</code>	1	1000	400	0
rv- <code>pareto-1.5</code>	3	(1000, 1000, 1000)	400	0
rv- <code>pareto-1.5</code>	3	(2000, 2000, 2000)	400	0
ebird and cloud	3	(0, 0, 0)	890	0
ebird and cloud	3	(1, 1, 1)	890	320
ebird and cloud	3	(2, 2, 2)	890	2134
ebird and cloud	3	(4, 4, 4)	890	16998

cloud is a real dataset containing 382 million cloud reports [15], each reporting time, latitude, longitude, and 25 weather attributes. ebird is a real dataset containing 508 million bird sightings, each with attributes describing time, latitude, longitude, species observed, and 1655 features of the observation site [27].

For each input, we explore different band widths as summarized in Table 1. *Output sizes below 0.5 million are reported as 0.* For the real data, the three join attributes are time ([days] since January 1st, 1970), latitude ([degrees] between  $-90$  and  $90$ ) and longitude ([degrees] between  $-180$  and  $180$ ).

**Local join algorithm.** After partitions are assigned to workers, each worker needs to locally perform a band-join on its partition(s). Many algorithms could be used, ranging from nested-loop to adaptations of IEJoin’s sorted arrays and bit-arrays. Since we focus on the *partitioning* aspect, the choice of local implementation is orthogonal, because it only affects the relative importance of optimizing for input duplication vs optimizing for max worker load. We observed that RECPART wins *no matter what this ratio is set to*, therefore in our experiments we selected a fairly standard local band-join algorithm based on index-nested-loops. (Let  $S_p$  and  $T_p$  be the input in partition  $p$ .) (1) range-partition  $T_p$  on  $A_1$  into ranges of size  $\epsilon_1$ . (Here  $A_1$  is the most selective dimension.) (2) For each  $s \in S_p$ , use binary search to find the  $T$ -range  $i$  containing  $s$ . Then check band condition on  $(s, t)$  for all  $t$  in ranges  $(i - 1)$ ,  $i$ , and  $i + 1$ .

Since GRID- $\epsilon$  partitions are of size  $\epsilon_1$  in dimension  $A_1$ , we slightly modify the above algorithm and sort both  $S_p$  and  $T_p$  on  $A_1$ . The binary search for  $s \in S_p$  then searches for  $s.A_1 - \epsilon_1$  (the smallest tuple  $t \in T_p$  it could join with) and scans the sorted  $T$ -array from there until  $s.A_1 + \epsilon_1$ .

**Statistics and running-time model.** We sample 100,000 input records and set output-sample size so that total time for statistics gathering does not exceed 5% of the fastest time (optimization plus join time) observed for any method. For output sampling we use the method introduced for CS<sub>IO</sub> [38]. For the cost model (see Section 2), we determine the model coefficients ( $\beta$ -values) as discussed in [24] from a benchmark of 100 queries. The benchmark is run offline once to profile the performance aspects of a cluster.

## 6.2 Impact of Band Width

We explore the impact of band width, which affects output. For comparison with grid partitioning, we turn RECPART’s symmetric partitioning off, i.e.,  $T$  is always the partitioned/duplicated relation. Since the grid approaches do not apply symmetric partitioning by design, all advantages of RECPART in the experiments are due to the better partition boundaries, not due to symmetric partitioning. (The impact of symmetric partitioning is explored separately later.) To avoid confusion, we refer to RECPART without symmetric partitioning as RECPART-S.

**6.2.1 Single Join Attribute.** The left block in Table 2a reports running times. RECPART-S wins in all cases, by up to a factor of 2, but the other methods are competitive because the join is in 1D and skew is moderate. For CS<sub>IO</sub> we tried different parameter settings that control optimization time versus partitioning quality, reporting the best found. The right block in Table 2a reports input plus duplicates ( $I$ ), and the input ( $I_m$ ) and output ( $O_m$ ) on the most loaded worker machine. Recall that profiling revealed  $\beta_2/\beta_3 \approx 4$ , i.e., each input tuple incurs 4 times the load compared to an output tuple.

RECPART-S and CS<sub>IO</sub> achieve similar load characteristics, because both intelligently leverage input and output samples to balance load while avoiding input duplication. However, RECPART-S finds a better partitioning (lower max worker load and input duplication) with 10x lower optimization time. The other two methods produce significantly higher input duplication, affecting  $I$  and  $I_m$ . GRID- $\epsilon$  still shows competitive running time because it works with a very fine-grained partitioning, i.e., each worker receives its input already split into many small grid cells. Data in a cell can be joined independent of the other cells, resulting in efficient in-memory processing. As a result, GRID- $\epsilon$  has lower per-tuple processing time than the other methods. (There each worker receives its input in a large “chunk” that needs to be range-partitioned.)

**6.2.2 Multiple Join Attributes.** Tables 2b and 2c show that the performance gaps widen when joining on 3 attributes: RECPART-S is the clear winner in total running time as well as join time alone. It finds the partitioning with the lowest max worker load, while keeping input duplication below 4%, while the competitors created up to 12x input duplication.

CS<sub>IO</sub> is severely hampered by the complexity of the optimization step. (Lowering optimization time resulted in higher join time due to worse partitioning.) GRID- $\epsilon$  suffers from  $O(3^d)$  input duplication in  $d$  dimensions. For 1-BUCKET, note that the numbers in Table 2a and Table 2b are virtually identical. This is due to the fact that it covers the entire join matrix  $S \times T$ , i.e., the matrix cover is not affected by the dimensionality of the join condition.

GRID- $\epsilon$  has by far the highest input duplication, but again recovers some of this cost due to its faster local processing that exploits that each worker’s input arrives already partitioned into small grid cells. This is especially visible when comparing to 1-BUCKET for band width (2, 2, 2) in Table 2c.

## 6.3 Skew Resistance

Table 3 investigates the impact of join-attribute skew, showing that RECPART-S handles it the best, again achieving the lowest max worker load with almost no input duplication. The competitors suffer from high input duplication; CS<sub>IO</sub> also from high optimization cost. Note that as skew increases, output size increases as well. This is due to the power-law distribution and the correlation of high-frequency join-attribute values in the two inputs. Greater output size implies a denser join matrix for CS<sub>IO</sub>, increasing its optimization time.

## 6.4 Scalability

Tables 4a to 4d show that RECPART-S and RECPART have almost perfect scalability and beat all competitors. In Tables 4a and 4b, from row to row, we double both input size and number of workers. In Table 4c, only the input size varies while the number of workers is constant. In Table 4d, we only change the number of workers. The latter two results are for an 8D band-join to explore which techniques can scale beyond dimensionality common today. For cost reasons, we use the running-time model to predict join time in Tables 4c and 4d. For queries on real data, the smaller inputs are random samples from the full data. Note that join output grows super-linearly, therefore perfect scalability cannot be achieved. Nevertheless, RECPART-S and RECPART come close to the ideal when taking the output increase into account. When the same query is run on different-sized clusters (Table 4d), RECPART scales out best. CS<sub>IO</sub>’s optimization time grows substantially as  $w$  increases. We explored various settings, but reducing optimization time resulted in even higher join time and vice versa. The numbers shown represent the

**Table 2: Impact of band width: RECPART-S wins in all cases, and the winning margin gets bigger for band joins with more dimensions. (Blue color highlights the main results; red color highlights a weak spot.)**

**(a) Pareto-1.5,  $d = 1$ , varying band width.**

Band width	Runtime (optimization time+join time) in [sec]				Relative time over RECPART-S			I/O sizes in [millions]: $I, I_m, O_m$											
	RECPART-S	CS <sub>IO</sub>	1-BUCKET	GRID- $\epsilon$	CS <sub>IO</sub>	1-BUCKET	GRID- $\epsilon$	RECPART-S	CS <sub>IO</sub>	1-BUCKET	GRID- $\epsilon$	RECPART-S	CS <sub>IO</sub>	1-BUCKET	GRID- $\epsilon$	RECPART-S	CS <sub>IO</sub>	1-BUCKET	GRID- $\epsilon$
0	351(3+348)	512(29+483)	762	—	1.46	2.17	N/A	400 14 83	496 13 131	2200 73 81	— — —	400 14 83	496 13 131	2200 73 81	— — —	400 14 83	496 13 131	2200 73 81	— — —
$10^{-5}$	539(7+532)	684(29+655)	1004	540	1.27	1.86	1.00	400 12 158	475 8 266	2200 73 153	800 27 153	400 12 158	475 8 266	2200 73 153	800 27 153	400 12 158	475 8 266	2200 73 153	800 27 153
$2 \cdot 10^{-5}$	813(3+810)	992(30+962)	1316	834	1.22	1.62	1.03	401 13 305	488 10 388	2200 73 304	800 27 304	401 13 305	488 10 388	2200 73 304	800 27 304	401 13 305	488 10 388	2200 73 304	800 27 304
$3 \cdot 10^{-5}$	878(3+875)	1170(30+1140)	1520	956	1.33	1.73	1.09	401 12 384	479 10 503	2200 73 376	800 27 376	401 12 384	479 10 503	2200 73 376	800 27 376	401 12 384	479 10 503	2200 73 376	800 27 376

**(b) Pareto-1.5,  $d = 3$ , varying band width.**

Band width	Runtime (optimization time+join time) in [sec]				Relative time over RECPART-S			I/O sizes in [millions]: $I, I_m, O_m$											
	RECPART-S	CS <sub>IO</sub>	1-BUCKET	GRID- $\epsilon$	CS <sub>IO</sub>	1-BUCKET	GRID- $\epsilon$	RECPART-S	CS <sub>IO</sub>	1-BUCKET	GRID- $\epsilon$	RECPART-S	CS <sub>IO</sub>	1-BUCKET	GRID- $\epsilon$	RECPART-S	CS <sub>IO</sub>	1-BUCKET	GRID- $\epsilon$
(0, 0, 0)	230(1+229)	366(46+320)	792	—	1.59	3.44	N/A	401 14 0	497 17 0	2200 73 0	— — —	401 14 0	497 17 0	2200 73 0	— — —	401 14 0	497 17 0	2200 73 0	— — —
(2, 2, 2)	344(2+342)	1339(694+645)	1149	1412	3.89	3.34	4.10	404 15 29	652 19 69	2200 73 37	5541 185 37	404 15 29	652 19 69	2200 73 37	5541 185 37	404 15 29	652 19 69	2200 73 37	5541 185 37
(4, 4, 4)	860(2+858)	2557(1345+1212)	1772	1816	2.97	2.06	2.11	413 14 290	838 31 321	2200 73 291	5485 183 291	413 14 290	838 31 321	2200 73 291	5485 183 291	413 14 290	838 31 321	2200 73 291	5485 183 291

**(c) Join of ebird with cloud,  $d = 3$ , varying band width.**

Band width	Runtime (optimization time+join time) in [sec]				Relative time over RECPART-S			I/O sizes in [millions]: $I, I_m, O_m$											
	RECPART-S	CS <sub>IO</sub>	1-BUCKET	GRID- $\epsilon$	CS <sub>IO</sub>	1-BUCKET	GRID- $\epsilon$	RECPART-S	CS <sub>IO</sub>	1-BUCKET	GRID- $\epsilon$	RECPART-S	CS <sub>IO</sub>	1-BUCKET	GRID- $\epsilon$	RECPART-S	CS <sub>IO</sub>	1-BUCKET	GRID- $\epsilon$
(0, 0, 0)	248(3+245)	346(38+308)	1418	—	1.40	5.72	N/A	890 30 0	951 32 0	4832 161 0	— — —	890 30 0	951 32 0	4832 161 0	— — —	890 30 0	951 32 0	4832 161 0	— — —
(1, 1, 1)	332(3+329)	1945(968+977)	1532	1419	5.86	4.61	4.27	895 35 5	1490 95 9	4832 161 11	10891 361 11	895 35 5	1490 95 9	4832 161 11	10891 361 11	895 35 5	1490 95 9	4832 161 11	10891 361 11
(2, 2, 2)	423(3+420)	2615(1553+1062)	1573	1377	6.18	3.72	3.26	899 32 66	1830 107 74	4832 161 67	10783 361 74	899 32 66	1830 107 74	4832 161 67	10783 361 74	899 32 66	1830 107 74	4832 161 67	10783 361 74

**Table 3: Skew resistance: RECPART-S is fastest and has much less data duplication than other methods. (Pareto- $z$ ,  $d = 3$ , band width (2, 2, 2), and increasing skew  $z = 0.5, \dots, 2$ .)**

Data Sets	Runtime (optimization time+join time) in [sec]				Relative time over RECPART-S			I/O sizes in [millions]: $I, I_m, O_m$											
	RECPART-S	CS <sub>IO</sub>	1-BUCKET	GRID- $\epsilon$	CS <sub>IO</sub>	1-BUCKET	GRID- $\epsilon$	RECPART-S	CS <sub>IO</sub>	1-BUCKET	GRID- $\epsilon$	RECPART-S	CS <sub>IO</sub>	1-BUCKET	GRID- $\epsilon$	RECPART-S	CS <sub>IO</sub>	1-BUCKET	GRID- $\epsilon$
pareto-0.5	230 (3+227)	609 (263+346)	1137	1146	2.65	4.94	4.98	401 13 0.3	577 20 1	2200 73 0.4	5582 186 0.4	401 13 0.3	577 20 1	2200 73 0.4	5582 186 0.4	401 13 0.3	577 20 1	2200 73 0.4	5582 186 0.4
pareto-1.0	290 (3+287)	1064 (525+539)	1235	1335	3.67	4.26	4.60	401 13 17	616 20 31	2200 73 14	5554 185 14	401 13 17	616 20 31	2200 73 14	5554 185 14	401 13 17	616 20 31	2200 73 14	5554 185 14
pareto-1.5	344 (2+342)	1339 (694+645)	1149	1412	3.89	3.34	4.10	404 15 29	652 19 69	2200 73 37	5541 185 37	404 15 29	652 19 69	2200 73 37	5541 185 37	404 15 29	652 19 69	2200 73 37	5541 185 37
pareto-2.0	485 (2+483)	1811 (1000+811)	1369	2417	3.73	2.82	4.98	406 14 111	747 19 168	2200 73 107	5522 184 107	406 14 111	747 19 168	2200 73 107	5522 184 107	406 14 111	747 19 168	2200 73 107	5522 184 107

best tradeoff found. GRID- $\epsilon$  failed on the largest synthetic input due to a memory exception caused by one of the grid cells receiving too many input records.

## 6.5 Optimizing Grid Size

Table 5 shows that grid granularity has a significant impact on join time, here model estimated, of GRID- $\epsilon$ . With the default grid size (2, 2, 2), join time is 9x higher compared to grid size (32, 32, 32), caused by input duplication. Our extension *GRID\** automatically explores different grid sizes, using the same running-time model  $\mathcal{M}$  as RECPART and CS<sub>IO</sub> to find the best setting. Starting with grid size  $\epsilon_i$  in dimension  $i$  for all join attributes  $A_i$ , it tries coarsening the grid to size  $j \cdot \epsilon_i$  in dimension  $i$ , for  $j = 2, 3, \dots$ . For each resulting grid partitioning  $\mathcal{G}$ , we execute  $\mathcal{M}(\mathcal{G})$  to let model  $\mathcal{M}$  predict the running time, until a local minimum is found.

Automatic grid tuning works well for Pareto- $z$  where both inputs are similarly distributed and band width is small: Lemma 3 applies with large  $c_1$  and small  $c_2$ , providing strong upper bounds on the amount of input in any  $\epsilon$ -range. This confirms that grid-partitioning can indeed work well for “sufficiently large” input even in 3D space. However, GRID\* fails on the reverse Pareto distribution as Table 6 shows. There  $S$  and  $T$  have very different density, resulting in small

$c_1$  and large  $c_2$ , and therefore much weaker upper bounds on the input per  $\epsilon$ -range. The resulting dense regions, as stated by Lemma 2, cause high input duplication and high input  $I_m$  assigned to the most loaded worker.

## 6.6 Comparing to Distributed IEJoin

Table 11 shows representative results for a comparison to the quantile-based partitioning used by IEJoin [19]. We explore a wide range of inter-quantile ranges (sizePerBlock) and report results for those at and near the best setting found. Note that RECPART can use the same local processing algorithm as IEJoin, therefore we are interested in comparing based on the quality of the partitioning, i.e.,  $I, I_m$ , and  $O_m$ . It is clearly visible that RECPART-S finds significantly better partitionings, providing more evidence that simple quantile-based partitioning of the join matrix does not suffice.

## 6.7 Impact of Local Join Algorithm

Table 8 shows a typical result of the impact of ratio  $\beta_2/\beta_1$ . A high ratio occurs in systems with fast data transfer and slow local computation. Replacing the local band-join algorithm with a faster one would lower the ratio. While the



**Table 4: Scalability experiments: REC PART-S and REC PART have almost perfect scalability and beat all competitors. (Dataset  $X/Y/w$  in (a) and (b) refers to  $X$  million input and  $Y$  million output on  $w$  workers.)**

**(a) Pareto-1.5,  $d = 3$ , band width (2, 2, 2).**

Data Sets	Runtime (optimization time+join time) in [sec]				Relative time over REC PART-S				I/O sizes in [millions]: $I, I_m, O_m$							
	REC PART-S	CS <sub>IO</sub>	1-BUCKET	GRID- $\epsilon$	CS <sub>IO</sub>	1-BUCKET	GRID- $\epsilon$		REC PART-S	CS <sub>IO</sub>	1-BUCKET	GRID- $\epsilon$				
200/282/15	306 (1+305)	1227 (767+460)	779	1381	4.01	2.55	4.51		202 13 20	290 19 36	800 53 19	2772	185	19		
400/1120/30	344 (2+342)	1374 (729+645)	1149	1412	3.99	3.34	4.10		404 15 29	652 19 69	2200 73 37	5541	185	37		
800/4460/60	438 (4+434)	1721 (801+920)	1731	FAILED	3.93	3.95	N/A		809 21 45	1690 42 74	6400 107 74	11089	185	74		

**(b) Join of ebird with cloud,  $d = 3$ , band width (2, 2, 2).**

Data Sets	Runtime (optimization time+join time) in [sec]				Relative time over REC PART-S				I/O sizes in [millions]: $I, I_m, O_m$							
	REC PART-S	CS <sub>IO</sub>	1-BUCKET	GRID- $\epsilon$	CS <sub>IO</sub>	1-BUCKET	GRID- $\epsilon$		REC PART-S	CS <sub>IO</sub>	1-BUCKET	GRID- $\epsilon$				
222/134/15	207 (3+204)	1213 (942+271)	547	812	5.86	2.64	3.92		223 15 11	307 22 11	856 57 9	2688	179	9		
445/530/30	193 (3+190)	1778 (1447+331)	688	771	9.21	3.56	3.99		448 16 14	748 26 27	2420 81 18	5403	180	18		
890/2000/60	215 (2+213)	1919 (1479+440)	1117	793	8.93	5.20	3.69		899 13 44	2040 38 35	6870 114 36	10805	180	36		

\* optimization time for 890/2000/60 is similar to that of 445/530/30 after we tuned parameters for CS<sub>IO</sub> s.t. it could finish optimization within 90 minutes.

**(c) Varying input size: pareto-1.5,  $d = 8$ , band width is 20 in each dimension, 30 workers.**

Input Size in [millions]	Join Result Size in [millions]	Runtime (optimization time+join time) in [sec]				I/O sizes in [millions]: $I, I_m, O_m$							
		REC PART	CS <sub>IO</sub>	1-BUCKET	GRID- $\epsilon$	REC PART	CS <sub>IO</sub>	1-BUCKET	GRID- $\epsilon$				
100	9	61 (5+56)	528 (449+79)	292	173,581	104 3 2	142 5 1	550 18 0.3	297,421	9,914	0.3		
200	57	120 (5+115)	612 (448+164)	587	347,944	210 7 2	285 10 5	1100 37 2	594,834	19,828	2		
400	219	240 (8+232)	760 (418+342)	1180	694,574	420 14 7	574 7 67	2200 73 7	1,189,996	39,667	7		
800	857	510 (17+493)	1166 (423+743)	2390	1.39 · 10 <sup>6</sup>	847 26 31	1180 53 4	4400 147 29	2,379,329	79,311	29		

**(d) Varying number of workers ( $w$ ): pareto-1.5,  $d = 8$ , band width is 20 in each dimension, input size 400 million.**

$w$	Join Result Size in [millions]	Runtime (optimization time+join time) in [sec]				I/O sizes in [millions]: $I, I_m, O_m$							
		REC PART	CS <sub>IO</sub>	1-BUCKET	GRID- $\epsilon$	REC PART	CS <sub>IO</sub>	1-BUCKET	GRID- $\epsilon$				
1		3655	3655	3655	8,527,502	400 400 219	400 400 219	400 400 219	1,189,996	1,189,996	219		
15	219	358 (5+353)	710 (190+520)	1295	1,040,000	420 28 10	565 40 29	1600 107 15	1,189,996	79,333	15		
30		240 (8+232)	760 (418+342)	1180	695,000	420 14 7	574 7 67	2200 73 7	1,189,996	39,667	7		
60		182 (10+172)	3703 (3431+272)	1287	525,000	425 6 5	619 13 2	3200 53 4	1,189,996	19,833	4		

**Table 5: GRID- $\epsilon$  vs. GRID\* on pareto-1.5, band width (2, 2, 2), varying grid size ( $I, I_m$  and  $O_m$  in [millions]).**

GRID- $\epsilon$					$I, I_m, O_m$ Join Time				
Grid Size	$I$	$I_m$	$O_m$	Join Time	GRID*				
(1,1,1)	5610	180	38	2993	460	16	46	335	
(2,2,2)	5541	185	37	3021	REC PART-S				
(4,4,4)	1780	60	38	1023	404	15	29	286	
(8,8,8)	861	29	38	533	CS <sub>IO</sub>				
(16,16,16)	582	20	39	389	652	19	69	459	
(32,32,32)	478	16	42	336	1-BUCKET				
(64,64,64)	435	15	56	344	2200	73	37	1236	

**Table 6: GRID\* vs. REC PART. I/O sizes in [millions].**

Data Sets	Band width	REC PART			GRID*			
		$I$	$I_m$	$O_m$	Grid Size	$I$	$I_m$	$O_m$
pareto-2.0	(2,2,2)	406	14	111	8	497	17	130
rv-pareto-1.5	(1K,1K,1K)	400	13	0	2750	882	237	0
rv-pareto-1.5	(2K,2K,2K)	401	13	0	11500	1207	401	0

competitors are not affected by the ratio (they all ignore network shuffle time), it is visible how *increasing weight on local join cost makes REC PART reduce max worker load*, incurring slightly higher input duplication.

**Table 7: Comparing to distributed IEJoin: Input duplication and max worker load on pareto-z,  $w = 30$ , varying skew and band width ( $I, I_m$  and  $O_m$  in [millions]).**

$Z$	Band width	Output size	REC PART-S			IEJoin			
			$I$	$I_m$	$O_m$	$I$	$I_m$	$O_m$	sizePerBlock
1.5	[0,0,0]	0	401	14	0	780	40	0	10000
						726	25	0	12524
						756	28	0	14000
1.5	[2,2,2]	1120	404	15	29	1092	48	14	6000
						1070	45	21	7422
						1062	36	85	9000
1.0	[2,2,2]	420	401	13	17	1176	40	21	4000
						1080	37	26	6263
						1088	48	4	8000
0.5	[2,2,2]	12	401	13	0.3	828	24	1	6000
						796	17	2	8295
						820	20	2	10000

## 6.8 Impact of Symmetric Partitioning

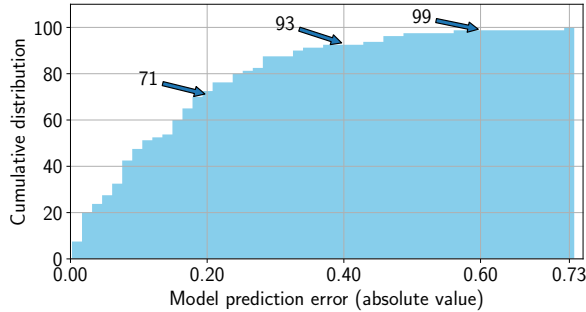
While REC PART and REC PART-S find similar partitionings on pareto-1.0 and the real data, the advantages of symmetric partitioning are revealed on the reverse Pareto data in Table 9. Here REC PART-S cannot split regions with high density of  $T$  without incurring high input duplication. In contrast, REC PART switches the roles of  $S$  and  $T$ , because  $S$  is sparse in those regions and hence the split creates few input duplicates.

**Table 8: Impact of local join algorithm: Input duplication  $I$  vs max worker load  $L_m = 4I_m + O_m$  for varying ratios  $\beta_2/\beta_1$  for join of ebird with cloud, band width (2, 2, 2),  $w = 30$ .**

$\beta_2/\beta_1$	RECPART		CS <sub>IO</sub>		1-BUCKET		GRID- $\epsilon$	
	$I$	$L_m$	$I$	$L_m$	$I$	$L_m$	$I$	$L_m$
0.0001	890.34	289						
0.001	890.36	223						
0.01	890.42	195						
0.1	890.52	191						
1	890.8	189	1830	502	4832	711	10800	1518
10	890.8	189						
100	890.8	189						
1000	890.8	189						
10000	890.8	189						

**Table 9: RECPART-S vs. RECPART (I/O sizes in [millions]).**

Data Sets	Band width	RECPART-S			RECPART		
		$I$	$I_m$	$O_m$	$I$	$I_m$	$O_m$
pareto-1.0	(2,2,2)	401	13	17	401	12	21
ebird and cloud	(0,0,0)	890	30	0	890	30	0
ebird and cloud	(2,2,2)	899	32	66	891	31	67
ebird and cloud	(4,4,4)	918	31	567	894	30	515
rv-pareto-1.5	(1000,1000,1000)	452	143	0	400	13	0
rv-pareto-1.5	(2000,2000,2000)	430	173	0	401	13	0
rv-pareto-1.5	2	433	40	0	401	14	0
rv-pareto-1.5	1000	402	200	0	402	14	0



**Figure 9: Accuracy of the running-time model: Cumulative distribution of model error.**

## 6.9 Accuracy of the Running-Time Model

In all experiments, the running-time model’s predictions were sufficiently accurate for identifying excellent partitionings for RECPART. Due to the high cost in terms of time and money of executing computations in the cloud, we sometimes rely on the running-time model also to report join time. Figure 9 shows the cumulative distribution of the relative error between predicted and measured join time for over 80 experiments selected randomly from all runs. E.g., the model has less than 20% error in over 70% of the cases and it is never off by more than a factor 1.8.

## 6.10 Near-Optimality of Our Approach

Figure 4 in Section 1 summarizes the results from all tables, making it easy to see how RECPART achieves significantly lower max worker load (y-axis) with less input duplication (x-axis). RECPART is always within 10% of the lower bound on both measures, beating the competition by a wide margin.

## 7 CONCLUSIONS

For distributed band-joins, we showed that recursive partitioning with the appropriate split-scoring measure achieves both low optimization time (a few seconds) and near-optimal join partitioning (within 10% of the respective lower bounds) on input duplication and max worker load. Even if system parameters change, e.g., due to faster networks or CPUs, RECPART’s achievement will still stand, because the issues of low input duplication and low input and output per worker will remain crucial optimization goals.

There are several exciting directions for future work. First, for band-joins between more than two relations, can one do better than reducing the problem to multiple two-way joins? Second, how do we partition for join conditions that contain a mix of various types of predicates, e.g., equality, inequality, band, and non-equality? Third, what other types of join conditions give rise to specialized methods, like RECPART for band-join, so that similarly significant improvements over generic theta-join approaches can be achieved?

More information about RECPART and other techniques for distributed data-intensive computations can be found at <https://northeastern-datalab.github.io/distributed/>.

## ACKNOWLEDGMENTS

This work was supported in part by the National Institutes of Health (NIH) under award number R01 NS091421 and by the National Science Foundation (NSF) under award number CAREER IIS-1762268. The content is solely the responsibility of the authors and does not necessarily represent the official views of NIH or NSF. We also would like to thank Aditya Ghosh for his contributions to design and implementation of GRID\*, Dhavalkumar Patel for implementing the join-sampling algorithm, and the anonymous reviewers and Niklas Smedemark-Margulies for their constructive feedback.

## REFERENCES

- [1] Paul Beame, Paraschos Koutris, and Dan Suciu. 2014. Skew in parallel query processing. In *PODS*. 212–223. <https://doi.org/10.1145/2594538.2594558>
- [2] Carsten Binnig, Andrew Crotty, Alex Galakatos, Tim Kraska, and Erfan Zamanian. 2016. The End of Slow Networks: It’s Time for a Redesign. *PVLDB* 9, 7 (2016), 528–539. <https://doi.org/10.14778/2904483.2904485>

- [3] Spyros Blanas, Jignesh M Patel, Vuk Ercegovic, Jun Rao, Eugene J Shekita, and Yuanyuan Tian. 2010. A comparison of join algorithms for log processing in mapreduce. In *SIGMOD*. 975–986. <https://doi.org/10.1145/1807167.1807273>
- [4] Nicolas Bruno, YongChul Kwon, and Ming-Chuan Wu. 2014. Advanced join strategies for large-scale distributed computation. *PVLDB* 7, 13 (2014), 1484–1495. <https://doi.org/10.14778/2733004.2733020>
- [5] Shumo Chu, Magdalena Balazinska, and Dan Suciu. 2015. From theory to practice: Efficient join query evaluation in a parallel database system. In *SIGMOD*. 63–78. <https://doi.org/10.1145/2723372.2750545>
- [6] Jeffrey Dean and Sanjay Ghemawat. 2008. MapReduce: Simplified Data Processing on Large Clusters. *Commun. ACM* 51, 1 (2008), 107–113. <https://doi.org/10.1145/1327452.1327492>
- [7] Hasanat M Dewan, Kui W Mok, Mauricio Hernández, and Salvatore J Stolfo. 1994. Predictive dynamic load balancing of parallel hash-joins over heterogeneous processors in the presence of data skew. In *PDIS*. 40–49. <https://doi.org/10.1109/PDIS.1994.331734>
- [8] David J DeWitt and Robert Gerber. 1985. Multiprocessor hash-based join algorithms. In *VLDB*. 151–164. <https://dl.acm.org/doi/10.5555/1286760.1286774>
- [9] David J DeWitt, Jeffrey F Naughton, and Donovan A Schneider. 1991. An evaluation of non-equi-join algorithms. In *VLDB*. 443–452. <https://dl.acm.org/doi/10.5555/645917.672320>
- [10] David J DeWitt, Jeffrey F Naughton, Donovan A Schneider, and Srinivasan Seshadri. 1992. Practical skew handling in parallel joins. In *VLDB*. 27–40. <https://dl.acm.org/doi/10.5555/645918.672512>
- [11] Jennie Duggan, Olga Papaemmanouil, Leilani Battle, and Michael Stonebraker. 2015. Skew-aware join optimization for array databases. In *SIGMOD*. 123–135. <https://doi.org/10.1145/2723372.2723709>
- [12] Mohammed Elseidy, Abdallah Elguindy, Aleksandar Vitorovic, and Christoph Koch. 2014. Scalable and adaptive online joins. *PVLDB* 7, 6 (2014), 441–452. <https://doi.org/10.14778/2732279.2732281>
- [13] Fabian Fier, Nikolaus Augsten, Panagiotis Bouros, Ulf Leser, and Johann-Christoph Freytag. 2018. Set Similarity Joins on MapReduce: An Experimental Survey. *PVLDB* 11, 10 (2018), 1110–1122. <https://doi.org/10.14778/3231751.3231760>
- [14] Paula Furtado and Peter Baumann. 1999. Storage of Multidimensional Arrays Based on Arbitrary Tiling. In *ICDE*. 480–489. <https://doi.org/10.1109/ICDE.1999.754964>
- [15] CJ Hahn, SG Warren, and R Eastman. 2012. Extended Edited Synoptic Cloud Reports from Ships and Land Stations Over the Globe, 1952–2009 (NDP-026C). (2012). <https://doi.org/10.3334/CDIAC/cli.ndp026c>
- [16] Jiawei Han, Jian Pei, and Micheline Kamber. 2011. *Data mining: concepts and techniques* (3rd ed.). Morgan Kaufmann. <https://doi.org/10.1016/C2009-0-61819-5>
- [17] Lilian Harada and Masaru Kitsuregawa. 1995. Dynamic Join Product Skew Handling for Hash-Joins in Shared-Nothing Database Systems.. In *DASFAA*. 246–255. <https://dl.acm.org/doi/10.5555/646710.703010>
- [18] Kien A Hua and Chiang Lee. 1991. Handling Data Skew in Multiprocessor Database Computers Using Partition Tuning. In *VLDB*. 525–535. <https://dl.acm.org/doi/10.5555/645917.672154>
- [19] Zuhair Khayyat, William Lucia, Meghna Singh, Mourad Ouzzani, Paolo Papotti, Jorge-Arnulfo Quiané-Ruiz, Nan Tang, and Panos Kalnis. 2017. Fast and scalable inequality joins. *VLDBJ* 26, 1 (2017), 125–150. <https://doi.org/10.1007/s00778-016-0441-6>
- [20] Masaru Kitsuregawa and Yasushi Ogawa. 1990. Bucket Spreading Parallel Hash: A New, Robust, Parallel Hash Join Method for Data Skew in the Super Database Computer (SDC). In *VLDB*. 210–221. <https://dl.acm.org/doi/10.5555/94362.94416>
- [21] Masaru Kitsuregawa, Hidehiko Tanaka, and Tohru Moto-Oka. 1983. Application of hash to data base machine and its architecture. *New Generation Computing* 1, 1 (1983), 63–74. <https://doi.org/10.1007/BF03037022>
- [22] Ioannis Koumarelas, Athanasios Naskos, and Anastasios Gounaris. 2018. Flexible Partitioning for Selective Binary Theta-joins in a Massively Parallel Setting. *Distrib. Parallel Databases* 36, 2 (2018), 301–337. <https://doi.org/10.1007/s10619-017-7214-0>
- [23] Usha Krishnamurthy. 2019. *Oracle Database SQL Language Reference 19c*. Oracle. <https://docs.oracle.com/en/database/oracle-database/19/sqlrf/index.html> Version 19.1.
- [24] Rundong Li, Ningfang Mi, Mirek Riedewald, Yizhou Sun, and Yi Yao. 2019. Abstract cost models for distributed data-intensive computations. *Distrib. Parallel Databases* 37, 3 (2019), 411–439. <https://doi.org/10.1007/s10619-018-7244-2>
- [25] Rundong Li, Mirek Riedewald, and Xinyan Deng. 2018. Submodularity of Distributed Join Computation. In *SIGMOD*. 1237–1252. <https://doi.org/10.1145/3183713.3183728>
- [26] HJ Lu and Kian-Lee Tan. 1994. Load-balanced join processing in shared-nothing systems. *J. Parallel and Distrib. Comput.* 23, 3 (1994), 382–398. <https://doi.org/10.1006/jpdc.1994.1148>
- [27] Arthur M Munson, Kevin Webb, Daniel Sheldon, Daniel Fink, Wesley M Hochachka, Marshall Liff, Mirek Riedewald, Daria Sorokina, Brian Sullivan, Christopher Wood, and Steve Kelling. 2014. The ebird reference dataset, version 2014. *Cornell Lab of Ornithology and National Audubon Society, Ithaca, NY* (2014). <https://ebird.org>
- [28] Alper Ocan and Mirek Riedewald. 2011. Processing Theta-joins Using MapReduce. In *SIGMOD*. 949–960. <https://doi.org/10.1145/1989323.1989423>
- [29] Orestis Polychroniou, Rajkumar Sen, and Kenneth A Ross. 2014. Track join: distributed joins with minimal network traffic. In *SIGMOD*. 1483–1494. <https://doi.org/10.1145/2588555.2610521>
- [30] Viswanath Poosala and Yannis E Ioannidis. 1996. Estimation of query-result distribution and its application in parallel-join load balancing. In *VLDB*. 448–459. <https://dl.acm.org/doi/10.5555/645922.673321>
- [31] Viswanath Poosala and Yannis E Ioannidis. 1997. Selectivity estimation without the attribute value independence assumption. In *VLDB*. 486–495. <https://dl.acm.org/doi/10.5555/645923.673638>
- [32] Viswanath Poosala, Yannis E. Ioannidis, Peter J. Haas, and Eugene J. Shekita. 1996. Improved Histograms for Selectivity Estimation of Range Predicates. In *SIGMOD*. 294–305. <https://doi.org/10.1145/233269.233342>
- [33] Wolf Rödiger, Sam Idicula, Alfons Kemper, and Thomas Neumann. 2016. Flow-join: Adaptive skew handling for distributed joins over high-speed networks. In *ICDE*. 1194–1205. <https://doi.org/10.1109/ICDE.2016.7498324>
- [34] Akash Das Sarma, Yeye He, and Surajit Chaudhuri. 2014. ClusterJoin: A Similarity Joins Framework using Map-Reduce. *PVLDB* 7, 12 (2014), 1059–1070. <https://doi.org/10.14778/2732977.2732981>
- [35] Donovan A Schneider and David J DeWitt. 1989. A performance evaluation of four parallel join algorithms in a shared-nothing multiprocessor environment. In *SIGMOD*. 110–121. <https://doi.org/10.1145/67544.66937>
- [36] Donovan A Schneider and David J DeWitt. 1990. Tradeoffs in processing complex join queries via hashing in multiprocessor database machines. In *VLDB*. 469–480. <https://dl.acm.org/doi/10.5555/645916.672141>
- [37] Valery Soloviev. 1993. A truncating hash algorithm for processing band-join queries. In *ICDE*. 419–427. <https://doi.org/10.1109/ICDE.1993.344039>
- [38] Aleksandar Vitorovic, Mohammed Elseidy, and Christoph Koch. 2016. Load balancing and skew resilience for parallel joins. In *ICDE*. 313–324. <https://doi.org/10.1109/ICDE.2016.7498250>
- [39] Christopher B Walton, Alfred G Dale, and Roy M Jenevein. 1991. A Taxonomy and Performance Model of Data Skew Effects in Parallel Joins.

- In *VLDB*. 537–548. <https://dl.acm.org/doi/10.5555/645917.672307>
- [40] Joel L. Wolf, Daniel M. Dias, Philip S. Yu, and John Turek. 1994. New algorithms for parallelizing relational database joins in the presence of data skew. *TKDE* (1994), 990–997. <https://doi.org/10.1109/69.334888>
  - [41] Yu Xu, Pekka Kostamaa, Xin Zhou, and Liang Chen. 2008. Handling data skew in parallel joins in shared-nothing systems. In *SIGMOD*. 1043–1052. <https://doi.org/10.1145/1376616.1376720>
  - [42] Matei Zaharia, Mosharaf Chowdhury, Michael J Franklin, Scott Shenker, and Ion Stoica. 2010. Spark: cluster computing with working sets. In *USENIX HotCloud*. <https://dl.acm.org/doi/10.5555/1863103.1863113>
  - [43] Xiaofei Zhang, Lei Chen, and Min Wang. 2012. Efficient Multi-way Theta-join Processing Using MapReduce. *PVLDB* 5, 11 (2012), 1184–1195. <https://doi.org/10.14778/2350229.2350238>
  - [44] Weijie Zhao, Florin Rusu, Bin Dong, and Kesheng Wu. 2016. Similarity Join over Array Data. In *SIGMOD*. 2007–2022. <https://doi.org/10.1145/2882903.2915247>



**Table 10: Band-join characteristics used in the experiments.** Input and output size are reported in [million tuples].

Data set	$d$	Band width	Input Size	Output Size
pareto-1.5	1	0	400	2430
pareto-1.5	1	$10^{-5}$	400	4580
pareto-1.5	1	$2 \cdot 10^{-5}$	400	9120
pareto-1.5	1	$3 \cdot 10^{-5}$	400	11280
pareto-1.5	3	(0, 0, 0)	400	0
pareto-1.5	3	(2, 2, 2)	400	1120
pareto-1.5	3	(4, 4, 4)	400	8740
pareto-0.5	3	(2, 2, 2)	400	12
pareto-1.0	3	(2, 2, 2)	400	420
pareto-2.0	3	(2, 2, 2)	400	3200
pareto-1.5	8	(20, ..., 20)	100	9
pareto-1.5	8	(20, ..., 20)	200	57
pareto-1.5	8	(20, ..., 20)	400	219
pareto-1.5	8	(20, ..., 20)	800	857
rv-pareto-1.5	1	2	400	0
rv-pareto-1.5	1	1000	400	0
rv-pareto-1.5	3	(1000, 1000, 1000)	400	0
rv-pareto-1.5	3	(2000, 2000, 2000)	400	0
ebird and cloud	3	(0, 0, 0)	890	0
ebird and cloud	3	(1, 1, 1)	890	320
ebird and cloud	3	(1, 1, 5)	890	1164
ebird and cloud	3	(2, 2, 2)	890	2134
ebird and cloud	3	(4, 4, 4)	890	16998
ptf_objects	2	$(2.78 \cdot 10^{-4}, 2.78 \cdot 10^{-4})$	1198	876
ptf_objects	2	$(8.33 \cdot 10^{-4}, 8.33 \cdot 10^{-4})$	1198	1125

## A ADDITIONAL EMPIRICAL RESULTS

We present additional measurements and insights from our empirical evaluation. Results from the main paper may be repeated here for convenience so that the reader can find relevant numbers in one place. Properties of the datasets used are summarized in Table 10.

### A.1 Comparing to Distributed IEJoin

Table 11 shows that REC<sub>PART</sub>-S has faster join time than the distributed version of IEJoin [19] for band joins.

IEJoin [19] uses a carefully designed data structure to speed up in-memory computation of joins with inequality predicates. Its distributed version sorts the input datasets on one of the join attributes and range-partitions them into default-sized blocks based on approximate quantiles, before pairs of joinable blocks are assigned to the  $w$  workers for local joining. We find that the block size, i.e., the granularity of the quantiles used to define the partitions in each input dataset, is a key meta-parameter. Table 11 shows how much it affects the efficiency of distributed band-joins. For each query, we search for the best block size and list a few smaller and larger ones. With a good block size, distributed IEJoin can have join time close to that of REC<sub>PART</sub>-S in certain cases. However, in most cases, it creates significantly higher input duplication than REC<sub>PART</sub>-S, thus having a longer join time. The higher duplication is caused by (1) partition boundaries that cut through dense input regions and (2) the direct use

of quantiles for defining partitions, instead of applying a covering algorithm to identify just  $w$  partitions (as CS<sub>IO</sub> [38] and M-Bucket-I [28] do). The main benefit of the covering algorithm is that it can often avoid duplication of input blocks that belong to multiple joinable block pairs by assigning those pairs to the same region in the cover.

### A.2 Accuracy of the Running-Time Model

Table 12 and Figure 9 show that our running-time model has a less than 20% relative error in over 70% of the cases. Table 13 sheds more light on how this model helps REC<sub>PART</sub> to intelligently choose which overhead to tune to improve join efficiency.

Table 12 lists the predicted and actual join time. Our running-time model predicts correctly which algorithm has shorter join time, and in most cases has a less than 20% relative error compared to the ground truth. Figure 9 summarizes the prediction errors in a cumulative distribution.

A major benefit of using a running-time model is to help REC<sub>PART</sub> determine which part of the distributed join computation has more impact on join time. Specifically, if the running-time model assigns a greater weight factor to total input size  $I$  than to the local overhead ( $4 \cdot I_m + O_m$ ), then REC<sub>PART</sub> will try to create less duplication, perhaps at the expense of a worse load balance. We conduct a series of experiments exploring how the weight factors in the running-time model affect REC<sub>PART</sub>. As shown in Table 13,  $\beta_1$  is fixed, and as  $\beta_2$  increases, the local overhead has a greater impact on the overall join time, so it is beneficial to reduce it. This is what REC<sub>PART</sub> does:  $I$  increases and  $4 \cdot I_m + O_m$  decreases as  $\beta_2$  gets bigger, indicating that the algorithm more aggressively partitions the data to reduce max worker load. The local join cost is proportional to the load  $4 \cdot I_m + O_m$ . The factor 4 here is obtained for our cluster using the method mentioned in [38].

### A.3 Benefits of Symmetric Partitioning

Table 14 shows that allowing to choose which of the inputs to duplicate across a split boundary (which is the benefit of REC<sub>PART</sub> over REC<sub>PART</sub>-S) can significantly reduce input duplication as well as the load on the most loaded worker machine at the same time, resulting in lower join time.

While the gap is small when high-density regions of both inputs coincide (pareto-z) or are sufficiently correlated (real data), the anti-correlated reverse Pareto distributions reveal the benefits of allowing more flexibility in the split decisions. In particular, REC<sub>PART</sub> is much better able to achieve near-perfect load balance with low input duplication, significantly lowering join time.

**Table 11: Appendix A.1: Comparing REC PART with distributed IEJoin on 30 workers. We use pareto data sets with 400 million input. The best block size (with the shortest join time) for each query is marked in bold. (Join result size,  $I$ ,  $I_m$  and  $O_m$  in [millions])**

Data Sets	Band Width	Join Result Size	REC PART-S			IEJoin					
			Join Time	$I$	$I_m$	$O_m$	Join Time	$I$	$I_m$	$O_m$	sizePerBlock
Pareto-1.5	[0,0,0]	0	229	401	14	0	523	780	40	0	10000
							551	770	44	0	11000
							391	726	25	0	12524
							406	754	26	0	13000
							422	756	28	0	14000
Pareto-1.5	[2,2,2]	1120	342	404	15	29	696	1092	48	14	6000
							707	1092	42	44	7000
							677	1070	45	21	7422
							695	1088	48	14	8000
							733	1062	36	85	9000
Pareto-1.5	[4,4,4]	8740	858	413	14	29	968	1088	64	900	16000
							922	1054	68	55	17000
							899	1116	72	19	18000
							3512	1064	38	1500	19000
							3753	1120	40	1610	20000
Pareto-1.0	[2,2,2]	420	287	401	13	17	670	1176	40	21	4000
							650	1120	40	18	5000
							635	1080	37	26	6263
							661	1106	42	18	7000
							676	1088	48	4	8000
Pareto-0.5	[2,2,2]	12	227	401	13	0.3	413	828	24	1	6000
							436	798	28	1	7000
							348	796	17	2	8295
							363	810	18	2	9000
							382	820	20	2	10000

**Table 12: Appendix A.2: Running-Time Model Accuracy. Unless stated otherwise, the join was executed on the 30-worker cluster. Dataset  $X/Y/w$  refers to input size of  $X$  million, output size of  $Y$  million and a cluster with  $w$  workers.**

Data Sets	Band Width	REC PART-S			CS <sub>IO</sub>			1-BUCKET			GRID- $\epsilon$		
		Predicted	Actual	Error	Predicted	Actual	Error	Predicted	Actual	Error	Predicted	Actual	Error
pareto-1.5, d=1	0	375.35	348	7.86%	491.55	483	1.77%	1323.69	762	73.71%	-	-	-
pareto-1.5, d=1	1.00E-05	507.36	532	-4.63%	711.22	655	8.58%	1464.09	1004	45.83%	722.61	540	33.82%
pareto-1.5, d=1	2.00E-05	807.54	810	-0.30%	969.48	962	0.78%	1758.54	1316	33.63%	1017.06	834	21.95%
pareto-1.5, d=1	3.00E-05	948.33	875	8.38%	1184.12	1140	3.87%	1898.94	1520	24.93%	1157.46	956	21.07%
pareto-1.5, d=3	(0,0,0)	215.13	229	-6.06%	265	320	-17.19%	1165.74	792	47.19%	-	-	-
pareto-1.5, d=3	(2,2,2)	286.53	342	-16.22%	462.5	645	-28.29%	1238.48	1149	7.79%	1379.65	1412	-2.29%
pareto-1.5, d=3	(4,4,4)	786.99	858	-8.28%	1090.11	1212	-10.06%	1733.19	1772	-2.19%	2211.65	1816	21.79%
ebird & cloud	(0,0,0)	331.96	245	35.49%	354.46	308	15.08%	1791.93	1418	26.37%	-	-	-
ebird & cloud	(1,1,1)	364.77	329	10.87%	787.67	977	-19.38%	1806.54	1532	17.92%	1456.17	1419	2.62%
ebird & cloud	(1,1,5)	459.77	432	6.43%	902.82	985	-8.34%	1844.18	1597	15.48%	1577.02	1505	4.79%
ebird & cloud	(2,2,2)	468.43	420	11.53%	1030.42	1212	-14.98%	1893.32	1573	20.36%	1717	1377	24.69%
pareto-0.5	(2,2,2)	210.255	227	-7.38%	313.74	346	-9.32%	1164.18	1137	2.39%	1260.7	1146	10.01%
pareto-1.0	(2,2,2)	242.82	287	-15.39%	382.77	539	-28.99%	1190.7	1235	-3.59%	1304.9	1335	-2.25%
pareto-1.5	(2,2,2)	282.63	342	-17.36%	461.91	645	-28.39%	1235.55	1149	7.53%	1379.65	1412	-2.29%
pareto-2.0	(2,2,2)	435.27	483	-9.88%	677.49	811	-16.46%	1372.05	1369	0.22%	2387.15	2417	-1.24%
pareto-1.5 200/282/15	(2,2,2)	249.48	305	-18.20%	375	460	-18.48%	882.45	779	13.28%	1327.65	1381	-3.86%
pareto-1.5 400/1120/30	(2,2,2)	282.63	342	-17.36%	461.91	645	-28.39%	1235.55	1149	7.53%	1379.65	1412	-2.29%
pareto-1.5 800/4460/60	(2,2,2)	469.98	434	8.29%	928.2	920	0.89%	2706.9	1731	56.38%	-	-	-
ebird & cloud 222/134/15	(2,2,2)	198.66	204	-2.62%	275.94	271	1.82%	693.27	547	26.74%	1216.96	812	49.87%
ebird & cloud 445/530/30	(2,2,2)	273.06	190	43.72%	457.41	331	38.19%	855.9	688	24.40%	778.77	771	1.01%
ebird & cloud 890/2000/60	(2,2,2)	235.746	213	10.68%	474.81	440	7.91%	1330.38	1117	19.10%	902.16	793	13.77%

#### A.4 Additional results for Section 6.2.2: “Multiple Join Attributes”

*Table 15 confirms the superiority of REC PART as dimensionality of the join condition increases.*

Compared to the results for 8-dimensional band conditions in Section 6.2.2, this series of experiments uses a smaller band width of 5 in each dimension, which results in significantly lower output size compared to band width 20 in each dimension. This helps CS<sub>IO</sub> because smaller output implies a less

Table 13: **Appendix A.2: Varying  $\beta_2$  in the running-time model “ $\beta_1 \cdot I + \beta_2 \cdot (4 \cdot I_m + O_m)$ ”, where  $\beta_1$  is fixed to be 1.0. The relative join time is calculated by dividing each join time by REC PART’s join time in the same row.**

**(a) Pareto-1.5, band width is (2, 2, 2), on 30 workers.**

$\beta_2$	REC PART		CS <sub>IO</sub>		1-BUCKET		GRID- $\epsilon$		Relative Join Time vs REC PART		
	$I$	$4 \cdot I_m + O_m$	$I$	$4 \cdot I_m + O_m$	$I$	$4 \cdot I_m + O_m$	$I$	$4 \cdot I_m + O_m$	CS <sub>IO</sub>	1-BUCKET	GRID- $\epsilon$
0.0001	401	2510							1.63	5.49	13.97
0.001	401	433							1.62	5.47	13.93
0.01	402	95							1.62	5.47	13.92
0.1	402	95							1.62	5.42	13.78
1	403	91	652	145	2200	329	5600	781	1.61	5.12	12.92
10	404	91							1.60	4.18	10.21
100	404	91							1.60	3.70	8.81
1000	404	91							1.59	3.63	8.61
10000	404	91							1.59	3.62	8.59

**(b) ebird joins cloud, band width is (2, 2, 2), on 30 workers.**

$\beta_2$	REC PART		CS <sub>IO</sub>		1-BUCKET		GRID- $\epsilon$		Relative Join Time vs REC PART		
	$I$	$4 \cdot I_m + O_m$	$I$	$4 \cdot I_m + O_m$	$I$	$4 \cdot I_m + O_m$	$I$	$4 \cdot I_m + O_m$	CS <sub>IO</sub>	1-BUCKET	GRID- $\epsilon$
0.0001	890.34	289							2.06	5.43	12.14
0.001	890.36	223							2.05	5.42	12.12
0.01	890.42	195							2.06	5.43	12.12
0.1	890.52	191							2.07	5.39	12.03
1	890.8	189	1830	502	4832	711	10800	1518	2.16	5.13	11.41
10	890.8	189							2.46	4.29	9.33
100	890.8	189							2.62	3.83	8.20
1000	890.8	189							2.65	3.76	8.04
10000	890.8	189							2.65	3.76	8.02

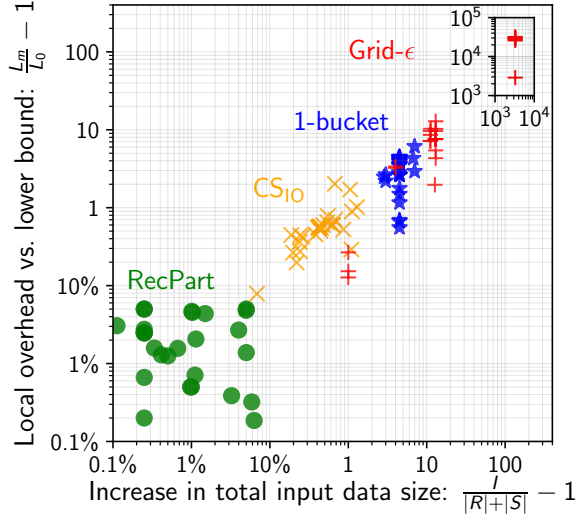


Figure 10: Total input duplication (x-axis) and maximum overhead across workers (y-axis) for our method REC PART vs. 3 competitors. In contrast to Figure 4, this figure additionally includes the data points from the appendix. As before, REC PART is always within 10% of the lower bounds (0% duplication and 0% overhead).

dense join matrix and hence lower optimization cost, but it still is significantly worse than REC PART.

### A.5 Results of REC PART using the theoretical termination condition

Table 16 shows that REC PART finds superior partitionings also when using the theoretical stopping condition that looks for the minimal overhead over the lower bounds on total input and max worker load. This does not rely on any cost model, except for an estimate of the relative cost per input vs per output tuple for the local join cost.

For this series of experiments, we used the Palomar Transient Factory (PTF) data set, which records observations of stars and galaxies. We explored join queries with an input of 1.198 billion records on two attributes: object right ascension and declination, with band width of 1 arc second ( $2.78 \cdot 10^{-4}$ ) and 3 arc seconds ( $8.33 \cdot 10^{-4}$ ), respectively. This type of queries finds pairs of celestial objects that are close to each other, helping the astronomers determine repeat observations of the same object. Table 16 shows total input including duplicates ( $I$ ), as well as max input and output size on the most loaded worker ( $I_m, O_m$ ). REC PART beats all competitors on all three measures, meaning it achieves both lower input duplication and max worker load.

### A.6 Near-Optimality of Our Approach

Figure 10 is a variant of Figure 4 summarizes the results from all tables including the ones from the appendix. We again see how REC PART achieves significantly lower max worker load (y-axis) with less input duplication (x-axis). REC PART is always within 10% of the lower bound on both measures, beating the competition by a wide margin.

**Table 14: Appendix A.3: RECPart-S vs. RECPart (Model-estimated join times in [sec], I/O sizes in [millions]).**

Data Sets	Band width	RECPart-S					RECPart					Ratio of RECPart join time to RECPart-S join time
		$I$	$I_m$	$O_m$	Imbalance	Join time	$I$	$I_m$	$O_m$	Imbalance	Join time	
pareto-1.0	(2,2,2)	401	13	17	1.02	243	401	12	21	1.02	242	1.00
ebird and cloud	(0,0,0)	890	30	0	1.01	332	890	30	0	1.01	332	1.00
ebird and cloud	(2,2,2)	899	32	66	1.03	434	891	31	67	1.02	429	0.99
ebird and cloud	(4,4,4)	918	31	567	1.09	1220	894	30	515	1.01	1038	0.93
reverse-pareto-2.0	(1000,1000,1000)	439	168	0	11.47	1429	425	19	0	1.32	261	0.18
reverse-pareto-2.0	(2000,2000,2000)	418	189	0	13.55	1584	475	19	0	1.18	275	0.17
reverse-pareto-2.0	2	458	34	0	2.21	387	413	19	0	1.36	258	0.25
reverse-pareto-2.0	1000	400	200	0	14.97	1666	550	33	0	1.82	409	0.67

**Table 15: Section 6.2.2 and Appendix A.4: Multidimensional joins on Pareto-1.5, varying dimension from 1 to 8 with band width 5 on each dimension. (Join time is estimated using the running-time model.)**

$d$	Join Result Size [millions]	Runtime (optimization time+join time) in [sec]				I/O sizes in [millions]: $I, I_m, O_m$							
		RECPart	CS <sub>IO</sub>	1-BUCKET	GRID- $\epsilon$	RECPart		CS <sub>IO</sub>		1-BUCKET		GRID- $\epsilon$	
1	$1.12 \cdot 10^8$	$6.77 \cdot 10^6$ ( $1+6.77 \cdot 10^6$ )	$9.4 \cdot 10^6$ ( $113+9.4 \cdot 10^6$ )	$7.27 \cdot 10^6$	$7.27 \cdot 10^6$	531	18 3470000	544	12 4820000	2200	73 3730000	785	27 3730000
2	313,000	20291 ( $1+20290$ )	26488 ( $113+26375$ )	21446	21340	409	12 10300	548	13 13400	2200	73 10400	1956	67 10400
4	860	266 (3+263)	519 (120+399)	1222	8751	406	11 34	573	27 19	2200	73 29	16004	547 29
8	0	217 (3+214)	458 (151+307)	1166	694560	404	14 0.0	560	20 0.00	2200	73 0	1280326	43747 0

**Table 16: Appendix A.5: RECPart using theoretical termination condition (I/O sizes in [millions]).**

Data Sets	Band Width	Join Result Size [millions]	RECPart			CS <sub>IO</sub>			1-BUCKET			GRID- $\epsilon$		
			$I$	$I_m$	$O_m$	$I$	$I_m$	$O_m$	$I$	$I_m$	$O_m$	$I$	$I_m$	$O_m$
ptf_objects	$(2.78 \cdot 10^{-4}, 2.78 \cdot 10^{-4})$	876	1198	39.98	29.08	1488	60.02	32.13	6589	220.00	29.20	5990	199.67	29.20
ptf_objects	$(8.33 \cdot 10^{-4}, 8.33 \cdot 10^{-4})$	1125	1198	40.25	36.39	1508	60.02	40.77	6589	220.99	37.50	5990	199.67	37.50